Differential Type I IFN-Inducing Abilities of Wild-Type versus Vaccine Strains of Measles Virus[1]

Masashi Shingai,[2]* Takashi Ebihara,* Nasim A. Begum,[3†] Atsushi Kato,[‡] Toshiki Honma,[‡] Kenji Matsumoto,[‡] Hirohisa Saito,[‡] Hisashi Ogura,[§] Misako Matsumoto,*[†] and Tsukasa Seya[4*†]

Laboratory adapted and vaccine strains of measles virus (MV) induced type I IFN in infected cells. The wild-type strains in contrast induced it to a far lesser extent. We have investigated the mechanism for this differential type I IFN induction in monocyte-derived dendritic cells infected with representative MV strains. Laboratory adapted strains Nagahata and Edmonston infected monocyte-derived dendritic cells and activated IRF-3 followed by IFN-β production, while wild-type MS failed to activate IRF-3. The viral IRF-3 activation is induced within 2 h, an early response occurring before protein synthesis. Receptor usage of CD46 or CD150 and nucleocapsid (N) protein variations barely affected the strain-to-strain difference in IFN-inducing abilities. Strikingly, most of the IFN-inducing strains possessed defective interference (DI) RNAs of varying sizes. In addition, an artificially produced DI RNA consisting of stem (the leader and trailer of MV) and loop (the GFP sequence) exhibited potential IFN-inducing ability. In this case, however, cytoplasmic introduction was needed for DI RNA to induce type I IFN in target cells. By gene-silencing analysis, DI RNA activated the RIG-I/MDA5-mitochondria antiviral signaling pathway, but not the TLR3-TICAM-1 pathway. DI RNA-containing strains induced IFN-β mRNA within 2 h while the same recombinant strains with no DI RNA required >12 h postinfection to attain similar levels of IFN-β mRNA. Thus, the stem-loop structure, rather than full genome replication or specific internal sequences of the MV genome, is required for an early phase of type I IFN induction by MV in host cells. *The Journal of Immunology,* **2007, 179: 6123–6133.**

The type I IFNs represent a family of soluble cytokines with biological and antiviral activity (1, 2). In acute-phase viral infection, IFNs are secreted from affected cells via activation of IFN-inducing signal pathways. Recently, how virus induces type I IFNs is a focus for investigation and it was found that virus nucleotides trigger activation of the intracellular molecular cascades for the IFN production. In vertebrates, nucleic acid-sensing receptors recognize viral nucleotides to induce the production of type I IFNs. Endosomal TLRs, TLR3 (3, 4), TLR7 (5, 6), and TLR9 (7), cytoplasmic PKR (8), and retinoic acid-inducible gene I (RIG-I)[5]-like RNA-recognition receptors (9, 10), function as viral RNA sensors and individually induce type I IFNs through their pathways. These pathways involve activation of IRF-3 transcription factor, which is crucial for promoter activation of IFN-β (1). Type I IFNs act in either an autocrine or paracrine fashion by inducing the expression of hundreds of genes that together establish an antiviral state, which restricts the spread of virus around neighboring cells. In addition, type I IFNs enhance the function of NK cells (11, 12) and the differentiation of virus-specific CTL (13). Although the exact mechanism by which these effectors are induced in virus-infected hosts remains unknown, this innate response to viral patterns triggers a various array of antiviral immunity and eliminate virus-infected cells.

Many viruses have developed mechanisms to circumvent the host antiviral responses, thus potentially augmenting early spread of virus (14, 15). Viral strategies include inhibition of cytoplasmic RNA sensors RIG-I or melanoma differentiation-associated gene 5 (MDA5), blocking IFN regulatory factor-3 (IRF-3)-activating signals of the IFN system, and interfering with IFNR response by modulating the JAK-STAT-1 pathway (14, 15). Viral proteins are known to associate these IFN-inhibitory modes (15). Some virus species may harbor other inhibitory modes for IFN production. In contrast, there appears a strain-to-strain difference in virus-mediated IFN-α/IFN-β induction. Low IFN-inducing viruses can actively suppress the IFN production of the high IFN-inducing strains. These findings have barely been analyzed in conjunction with the various inhibitory modes of virus molecules and host receptors for IFN signaling.

*Department of Microbiology and Immunology, Graduate School of Medicine, Hokkaido University, Sapporo, Japan; †Department of Immunology, Osaka Medical Center for Cancer, Osaka, Japan; ‡Department of Allergy and Immunology, National Research Institute for Child Health and Development, Tokyo, Japan; and §Department of Virology, Osaka City University, Osaka, Japan

Received for publication February 12, 2007. Accepted for publication July 27, 2007.

The costs of publication of this article were defrayed in part by the payment of page charges. This article must therefore be hereby marked *advertisement* in accordance with 18 U.S.C. Section 1734 solely to indicate this fact.

[1] This work was supported in part by CREST and Innovation, Japan Science and Technology Corporation, and by Grants-in-Aid from the Ministry of Education, Science, and Culture (Specified Project for Advanced Research), and the Hepatitis C Virus Project in National Institutes of Health of Japan, and by the Takeda Foundation, the Uehara Memorial Foundation, the Mitsubishi Foundation, the Akiyama Foundation, and the NorthTec Foundation.

[2] Current address: National Institute of Allergy and Infectious Diseases, National Institutes of Health, Bethesda, MD 20892.

[3] Current address: Department of Molecular Biology, Graduate School of Medicine, Kyoto University, Kyoto, Japan.

[4] Address correspondence and reprint requests to Dr. Tsukasa Seya, Department of Microbiology and Immunology, Graduate School of Medicine, Hokkaido University, Kita-ku, Sapporo 060-8638 Japan. E-mail address: seya-tu@pop.med.hokudai.ac.jp

[5] Abbreviations used in this paper: RIG-I, retinoic acid-inducible gene; MDA5, melanoma differentiation-associated gene 5; IRF, IFN regulatory factor; MV, measles virus; p.i., postinfection; mDC, myeloid DC; DI, defective interference; CHO, Chinese hamster ovary; pAb, polyclonal Ab; MOI, multiplicity of infection; siRNA, small interference RNA; TBK1, TANK-binding kinase 1; IKKε, IκB kinase-related kinase ε; MAVS, mitochondria antiviral signaling; ISRE, IFN-stimulated response element; Q-PCR, quantitative PCR; NAP1, NAK-associated protein 1; CIAP, calf intestine alkaline phosphatase; SeV, Sendai virus; VISA, virus-induced signaling adaptor.

In measles virus (MV), wild-type strains barely induce production of significant quantities of IFN-α/IFN-β (16). In contrast, measles vaccine strains, including the attenuated Edmonston (ED) strain, are efficient IFN inducers that cause part of the attenuation of virulence. The wild-type MV strains actually suppress IFN production induced by coinfected MV ED infection (16). Furthermore, 10 passages of the wild-type MVs on Vero cells are sufficient to transform their phenotype from an IFN suppressor to an IFN inducer (16). These earlier studies stressed the total output of IFN production, measuring the IFN-α/IFN-β content >24 h postinfection (p.i.; late phase), thus the event involving replication and translation of viral genome RNA. Yet, the possible participation of viral V and C proteins in the IFN production has not been sufficiently considered under the contemporary knowledge (15). The molecular basis of strain-specific IFN-inducing ability, therefore, remains largely undetermined.

We have compared the IFN-α/IFN-β induction and sensitivity of the laboratory passaged attenuated MV strains with those of recent wild-type viruses isolated and passaged on human PBMC, the B95a marmoset B cell line, or early passage lots of Vero cells. We found that the majority of vaccine and laboratory adapted MV strains rapidly induced the IFN-β mRNA within 12 h p.i. (early phase) independent of viral protein translation. A further finding was that the robust production of IFN-β in human myeloid dendritic cells (mDCs) and epithelial cells paralleled the elevating of the level of virus-specific defective interfering RNA (DI RNA). The DI RNAs are subviral replicons originating from the viral genome and are associated with many RNA viruses (17). Wild-type MV isolates induced significantly lower production of IFN in mDCs and they contained undetectable levels of DI RNA. Thus, we speculate that DI RNA in MV isolates is a crucial determinant for high IFN induction in MV laboratory adapted and vaccine strains.

Materials and Methods

Cell culture and reagents

The human lung epithelial cell line (A549), A549/CD150, African green monkey kidney cell line (Vero), Vero/CD150, HEK293, and 293-3-46 cells (kindly provided by M. A. Billeter, University of Zurich, Zurich, Switzerland) were maintained in DMEM supplemented with 10% heat-inactivated FCS (JRH Biosciences) and antibiotics. Chinese hamster ovary (CHO), CHO/CD46, and CHO/CD150 (18) were cultured in Eagle's MEM with 5% heat-inactivated FCS. B95a cells were grown in RPMI 1640 supplemented with 5% heat-inactivated FCS and antibiotics. Cells were kept in 5% CO_2 at 37°C incubator. Vero/CD150 was established according to the method by Ono et al. (19). For establishing CD150-expressing A549 and Vero sublines, $pCNX_2$-huCD150, an expression plasmid for human CD150 bearing a neomycin-resistance gene was introduced into A549 cells using Lipofectamine 2000 (Invitrogen Life Technologies) according to the manufacturer's recommendation. Two days after transfection, the neomycin analog G418 (Sigma-Aldrich) was added to the medium at the final concentration of 1 or 2 mg/ml for A549 or Vero cells. During the selection, G418-containing medium was changed once every 4 days. G418-resistant, stably transfected clones were propagated for the study of surface expression of CD150 by FACS. Poly I:C was purchased from Amersham. Mouse mAbs against human CD150 (IPO-3) was purchased from eBioscience and mAbs against human CD46 (M75 and M177) were produced in our laboratory (20). Rabbit polyclonal Ab (pAb) against human CD150 or human CD46 was produced in our laboratory (21). HRP-conjugated goat anti-rabbit Igs were obtained from American Qualex Manufacturers.

Virus preparation and titration

Nagahata (NV) and Edmonston (ED) strains were obtained from the Research Institute for Microbial Diseases (Osaka University, Osaka, Japan) and University of Washington (Seattle, WA), respectively. Ichinose (IC)-B and IC-V were provided from Drs. F. Kobune (National Institutes of Health, Tokyo, Japan) and K. Takeuchi (Tsukuba University, Tsukuba, Japan) (22). Wild-type MV strains were from Osaka University, Osaka City University, and Osaka Prefectural Research Institute. Masusako (MS) and other strains of MV were propagated in our laboratory (21, 23, 24). Vaccine strains of MV were purchased from Takeda, Tanabe, and Banyuu (Osaka, Japan). ED, NV, IC-V, MS, Yokota, CAM, AIK-C, Schwarz, and Tanabe strains were maintained in Vero cells in our laboratory. MS and Yokota strains are early passage lots (<10 passages). IC-B, Na-PBMC, Suz-PBMC, MOE, HY, Moka, and Kishida strains were maintained in B95a cells as reported (22). Virus titer was determined as PFUs on Vero/CD150 and the multiplicity of the infection (MOI) of each experiment was calculated based on this titer (19). For Ab blocking of measles virus entry receptors, cells were pretreated with pAb (35 μg/ml) against human CD46 or human CD150, or mAb (5 μg/ml) against human CD150 or human CD46 for 1 h before the virus infection (25).

Preparation of human monocyte-derived immature dendritic cells and macrophages

Human PBMC were isolated from buffy coat of normal healthy donors by methylcellulose sedimentation followed by standard density gradient centrifugation with Ficoll-Hypaque (Amersham Bioscience) (26). For human immature mDC and macrophage preparations, $CD14^+$ monocytes were obtained from human PBMC by using MACS system (Miltenyi Biotec) with anti-human CD14 mAb-conjugated microbeads. For mDCs, $CD14^+$ monocytes were kept in RPMI 1640 containing 10% FCS, 500 IU/ml human GM-CSF, 100 IU/ml human IL-4 (PeproTech) and antibiotics for 6 days. For macrophages, $CD14^+$ monocytes were kept in RPMI 1640 containing 10% FCS, 500 IU/ml human GM-CSF, and antibiotics for 9 days. Morphological changes were examined by phase contrast microscopy (Olympus IX-70).

Determination of human IFN-β level

For the estimation of secreted IFN-β, culture medium were centrifuged to remove cell debris and the supernatants were stored at −80°C until the assay. The level of secreted human IFN-β in the culture medium was determined according to the manufacturer's protocol using ELISA kit (Fujirebio).

FACS cytometric analysis of cell surface Ags

Methods for FACS analyses were described previously (26). Briefly, cells were suspended in PBS containing 0.1% sodium azide and 1% BSA (FACS buffer) and incubated for 30 min at 4°C with anti-CD46, CD150, or isotype control, washed, followed by FITC-labeled anti-mouse IgG $F(ab')_2$. Cells were washed and fluorescence intensity was measured by FACS.

Expression profile analysis with GeneChip

All microarray experiments and their data were analyzed according to Minimum Information About a Microarray Experiment (MIAME) guidelines. Total RNA from mDCs was extracted by the RNeasy kit (Qiagen) according to the manufacturer's instructions. Total RNA (10 μg) from each sample was used to prepare cRNA. Gene expression was analyzed with GeneChip Human Genome U133A probe array (Affymetrix), which contains ~22,000 gene probe sets. Data analysis was performed with Affymetrix microarray suite software version 5 (MAS 5.0; Affymetrix) and GeneSpring software version 6.1 (Silicon Genetics). The default settings of MAS 5.0 were used to calculate scaled gene expression values for each sample.

Native PAGE, SDS-PAGE, and Western blotting

Whole cell extracts were prepared in 20 mM HEPES containing 25% (v/v) glycerol, 0.42 M NaCl, 1.5 mM $MgCl_2$, 0.2 mM EDTA, 0.5 mM PMSF, 0.5 mM DTT, 30 mM NaF, and 1 mM Na_3VO_4. Protein concentration of the lysate was measured by Bio-Rad protein assay kit. For detection of phosphorylated IRF-3, whole cell extracts (60 μg) were subjected to SDS-PAGE in a 7.5% polyacrylamide gel. Proteins were electrophoretically transferred to Immobilon-P (Millipore) and probed with 1/500 diluted anti-IRF-3 pAb (FL-425; Santa Cruz Biotechnology). Dimer formation of IRF-3 was observed by separating the cell extracts (20 μg) on 7.5% polyacrylamide gel native PAGE (Dai-ichi Pure Chemicals), transferred to membrane, and probed with anti-IRF-3 pAb (1/100 diluted; IBL), washed with PBS containing 0.5% Tween 20 three times and incubated with HRP-conjugated goat anti-rabbit Ig pAb for 1 h at 37°C. Following second incubation, the membranes were washed three times with PBS-Tween 20 and proteins were detected with an ECL chemiluminescence kit (Amersham Biosciences) (26).

RT-PCR and quantitative PCR (Q-PCR)

To remove the viruses attached on cell surface, cells were treated with trypsin, neutralized with serum containing medium, and washed three

Table I. *Cellular responses to various strains of MV*

Strains	IFN-β Production[a]	Syncytium[b]					Passage
	DCs	DCs	Mϕ	CHO	CHO/CD46	CHO/CD150	
Laboratory adapted strains							
ED	+	++	+	−	+++	+++	Vero
NV	++	+	+	−	++	++	Vero
IC-V	+	+	+	−	+	++	Vero
Wild-type strains							
MS	−	++	−	−	−	+++	Vero**
Yokota	−	++	−	−	−	+	Vero**
IC-B	−	++	−	−	−	+	B95a
Na-PBMC	−	++	−	−	−	+	B95a
Suz-PBMC	−	++	−	−	−	+	B95a
MOE	−	++	−	−	−	++	B95a
HY	−	++	−	−	−	++	B95a
Moka	−	++	−	−	−	++	B95a
Kishida	−	++	−	−	−	+	B95a
Vaccine strains							
CAM	+	+	+*	−	+	++	Vero
AIK-C	+	+	+*	−	+	++	Vero
Schwarz	+	+	+*	−	+	++	Vero
Tanabe	++	++	+*	−	+	++	Vero

[a] ++, >10 IU/ml; +, <10 IU/ml.
[b] +++, >60% CPE; ++, 30–60% CPE; +*, aggregated (atypical CPE); **, virus replicates in cells without syncytium formation; −, not detected.

times with ice-cold PBS. Total RNA was extracted with RNeasy mini kit (Qiagen), 2 μg of total RNA was incubated at 70°C for 5 min, kept on ice for 2 min, and reverse transcription was performed with Moloney murine leukemia virus-reverse transcriptase (Promega) at 37°C for 90 min followed by PCR or Q-PCR. For PCR, ex-*Taq*DNA polymerase (Takara) was used. Sequences of the primers used for RT-PCR were reported earlier (27). Reaction for Q-PCR was performed with iQ SYBER Green Supermix and amplified PCR products were measured by iCycler iQ real-time PCR analyzing system (Bio-Rad). Primers for PCR were designed using Primer Express software (PerkinElmer/Applied Biosystems). The following primers were used for Q-PCR: human β-actin forward, 5′-CCTGGCACCCA GCACAAT-3′; reverse, 5′-GCCGATCCACACGGAGTACT-3′; human IFN-β forward, 5′-CAACTTGCTTGGATTCCTACAAAG-3′; reverse, 5′-TATTCAAGCCTCCCATTCAATTG-3′; MV-H-forward 5′-CCCTTATC AACGGATGATCC-3′; reverse-5′-GTGATCAATGGCCCGAATCC-3′. Normalized value for each mRNA expression was calculated as relative quantity of mRNA divided by the relative quantity of human β-actin.

RNA interference

The method for gene-silencing using small interference RNA (siRNA) oligonucleotides was described previously (28). The method for transient gene-silencing using siRNA oligonucleotides was described previously (29). The sequences of the siRNA for TICAM-1 (29), TANK-binding kinase 1 (TBK1), IκB kinase-related kinase ε (IKKε) (30), RIG-I, MDA5, and mitochondria antiviral signaling (MAVS) (IPS-1/Cardif/VISA) (31) were reported previously. The method for establishing stable gene-silenced HeLa cells was reported in a preceding report (28). Knockdown status was analyzed by RT-PCR.

Reverse genetics to produce recombinant MV

MV323 (wild-type Ichinose strain) and MV2A (ED strain) were recovered from p^+MV323 and p^+MV2A, respectively, as previously described (27, 32). Briefly, 293-3-46 cells were transfected with p^+MV323 and p^+MV2A, plus L gene-expressing plasmid. Two days later, B95a cells were overlaid. Recovered viruses were amplified with Vero or Vero/CD150 cells.

p(−) MV minigenome replicon GFP and in vitro transcription of the RNA replicon

The vector p(−)MV minireplicon GFP was constructed for transcribing the MV minireplicon GFP RNA(−) as a MV short genome. MV minireplicon GFP RNA contains the leader sequence, noncoding region of the N gene, GFP gene, noncoding region of the L gene, and the trailer sequence. The cDNA of MV minireplicon GFP was inserted into pT7 MV vector (containing T7 promoter, T7 terminator, genomic hepatitis δ virus ribozyme) which was constructed by modifying p^+MV323 (provided Dr. K. Takeuchi, Tsukuba University) (32). MV minireplicon GFP RNA^- was transcribed from p^-MV minireplicon GFP RNA^+ using MEGAscript T7 kit (Ambion) in vitro. Calf intestine alkaline phosphatase (CIAP; Takara) treatment of the transcribed RNA was performed according to the manufacturer's protocol.

Plasmid transfection and luciferase assay

A luciferase reporter gene plasmid, pISRE-Luc (firefly luciferase, experimental reporter), was purchased from Stratagene, pRL-TK vector (*Renilla* luciferase for internal control) was obtained from Promega. All transfections were conducted on HEK293 cells growing in 24-well plates. Usually, 100 ng of pISRE-Luc and 3 ng of pRL-TK vector were introduced into cells according to the manufacturer's procedure (Qiagen). At 24 h posttransfection, synthetic MV minireplicon RNA or poly I:C was introduced into cells by Lipofectamine 2000 (Invitrogen Life Technologies). Six hours later, cells were harvested with trypsin, washed with PBS, and treated with 20 μl of passive lysis buffer (Promega) and the assay was performed using dual luciferase reporter assay system (26). Fold induction against the control medium is indicated.

RT-PCR amplification of cDNA from 5′ copy-back DI RNAs

We modified the RT-PCR amplification protocol of Calain (33), where the copy-back DI RNAs were amplified using two sets of MV primers (for 5′ copy-back DIs, JM396; 5′-TATAAGCTTACCAGACAAAGCT GGGAATAGAAACTTCG-3′/JM403; 5′-CGAAGATATTCTGGTGTA AGTCTAGTA-3′, and for standard genome, JM396/JM402; 5′-TTTA TCCAGAATCTCAARTCCGG-3′) (34, 35). Viral RNA from the culture supernatant was extracted with QIAamp Viral RNA Mini kit (Qiagen). Total RNA from viral-infected cells was extracted with the RNeasy mini kit (Qiagen). Two micrograms of total RNA was incubated at 70°C for 5 min, kept on ice for 2 min, and reverse transcription was performed with Moloney murine leukemia virus-reverse transcriptase (Promega) at 37°C for 90 min followed by PCR. The PCR-amplified products were cloned into pCR blunt vector (Invitrogen Life Technologies) and sequencing was performed using the BigDye Terminator version 3.1 Cycle Sequencing kit (Applied Biosystem).

Results

MV attenuated strains induce IFN-β in mDC infection

Type I IFN-inducing activity of various MV strains was tested using mDCs by ELISA (Table I). Laboratory adapted strains ED, NV, and IC-V, and vaccine strains CAM, AIK-C, Schwarz, and Tanabe, all produced IFN-β in infected mDCs. These stains were propagated through Vero cells. CHO cells expressing either CD46

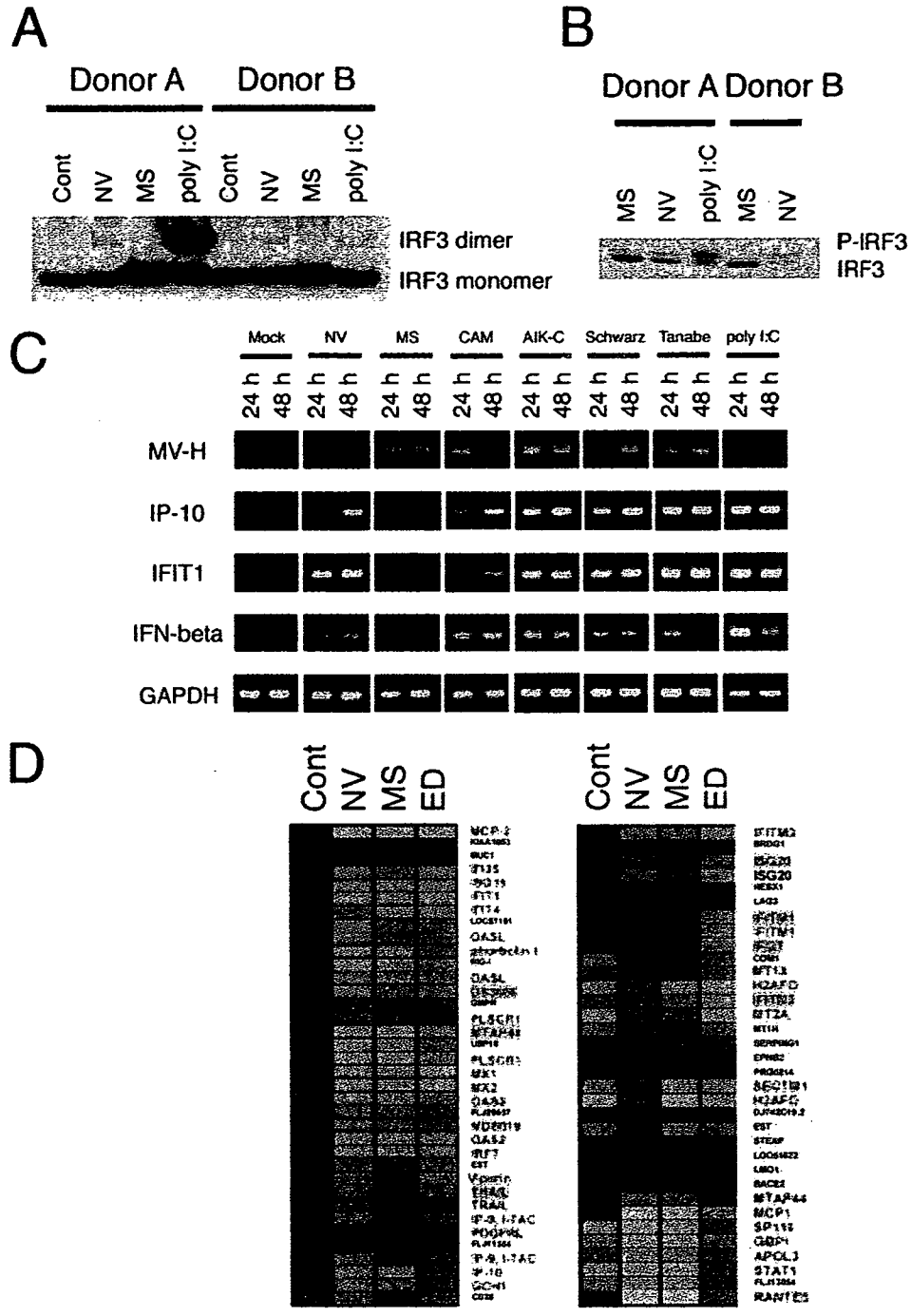

FIGURE 1. Laboratory adapted and vaccine strains highly induce type I IFN and IFN-inducible genes in monocyte-derived mDCs. Monocyte-derived mDCs were stimulated with medium alone (cont), poly I:C (10 μg/ml for 1 h), or MV strains (MOI = 1 typically for 8 h). At timed intervals, cells were lysed for IRF-3 analysis. CD46-adapted strain (NV or ED), CD46 nonadapted strain (MS), or vaccine strains (CAM, AIK-C, Schwarz, or Tanabe). *A*, Native gel analysis for IRF-3 dimerization; or *B*, SDS-PAGE for IRF-3 phosphorylation. *C*, At indicated intervals, MV-H, IP-10, IFIT1, IFN-β, and GAPDH mRNAs were detected using RT-PCR. *D*, Three major clusters of MV-regulated genes in mDCs infected with various MV strains. mDCs were infected with the indicated MV strains at MOI = 1. 8 h later, RNAs were extracted from the mDCs and analyzed by GeneChip. Data were analyzed by applying a hierarchical-tree algorithm to the normalized intensity. Induced genes are indicated by shades of red; repressed genes are indicated by shades of blue. Gene symbols are shown in the *right column*.

or CD150 formed syncytia when infected with these strains (Table I). In contrast, wild-type isolates largely established in Osaka were mostly passaged with B95a cells and barely produced IFN-β. Only CHO cells expressing CD150 formed syncytia by wild-type MV infection. Because the results on the receptor usage of these strains are consistent with ability of type I IFN induction, MV adaptation to the CD46 receptor might have linked the high IFN-inducing phenotype.

Defective IRF-3 activation in low IFN inducers of wild-type strains

Activation of IRF-3 was tested with human mDCs using representative laboratory adapted (NV, ED) and a Vero-adapted wild-type (MS) strain. NV and ED but not wild-type strain MS induced dimerization (Fig. 1*A*) and phosphorylation (Fig. 1*B*) of IRF-3. The results were confirmed with other laboratory adapted, vaccine, and wild-type strains (data not shown). Thus, strain-specific IRF-3 activation determines IFN-β induction in mDCs. NV and vaccine strains induced IFN-inducible genes, *IP-10*, *IFIT1*, and *IFN-β*, but the wild-type-strain including MS did not (Fig. 1*C*). An example of our comprehensive approaches regarding type I IFN-inducible genes are shown by microarrays using mRNAs from immature mDCs infected with representative strains (Fig. 1*D*). NV and ED strains, but not the MS strain, up-regulated IFN-inducible genes, supporting their high vs low IFN-β-inducing properties.

What factor is responsible for high IFN-β-inducing properties in MV?

The findings in Fig. 1 allowed us to surmise that NV and ED contain a factor that is responsible for higher induction of IFN-β

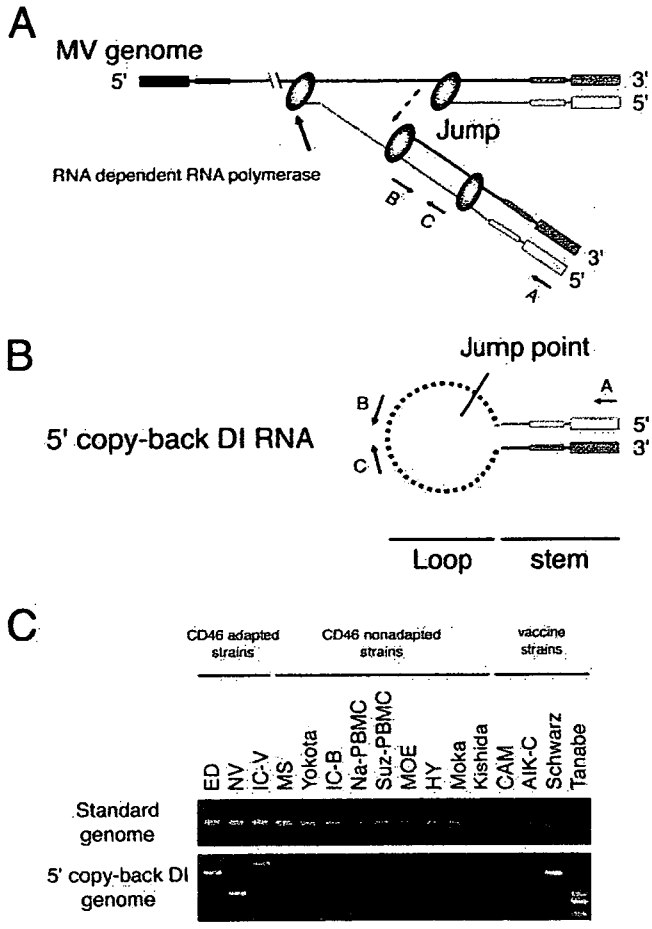

FIGURE 2. Laboratory adapted and vaccine strains contain 5′ copy-back DI RNA. *A*, Model for the origin of 5′ copy-back DI RNA. Two RNA polymerase complexes synthesized a negative-strand RNA from the positive-strand RNA template. The polymerase complex switches the template to a negative-strand RNA synthesized by a front RNA complex. *B*, The product perfectly matches with a part of the terminal and RNA duplex (stem). *C*, RT-PCR amplification of 5′ copy-back DI RNA from various strains of MV culture supernatants. RT-PCR was performed using standard genome-specific primers (primer A, JM396; and primer B, JM402, in the *upper panel*) or DI-specific primers (primer A, JM396; and C, JM403, in the *lower panel*).

and MS and other wild-type strains lack it. Then, the question is what factor participates in high IFN-β induction in MV laboratory adapted strains. NV and ED, but not MS, use CD46 as an entry receptor (18, 21). Both stimulation and mAb-blocking studies on the receptor CD46 suggested no direct participation of CD46 in IFN-β induction (M. Taniguchi and T. Seya, unpublished data). A previous report suggested the involvement of nucleocapsid (N) protein of MV in IFN induction (36, 37). Transfectants with N protein, however, did not induce IFN promoter activation (M. Shingai and T. Seya, unpublished data). N protein-expressing cells further transfected with MV RNA elevated IFN promoter activation compared with mock transfection with RNA alone (data not shown). Thus, these previous findings did not explain the differential induction of IFN-β in wild-type vs vaccine strains upon infected cells. Because the IFN-inducing ability of NV was dominant in cells coinfected with MS in an early phase, IFN-inducing rather than IFN-inhibitory factors (38) govern the IFN-inducing phenotype of MV in the early phase.

Our repetitive trials suggested that 5′ copy-back DI RNA has the ability to induce IFN-β. 5′ copy-back DI RNA was present in most of the laboratory adapted and vaccine strains (Fig. 2*A*). By using the method of Calain and others (33–35), a unique primer set enabled us to detect 5′ copy-back DI RNA by RT-PCR (Fig. 2, *A* and *B*). Standard genome-specific primers are primer A (JM396) and B (JM402). DI RNA-specific primers are: primer A (JM396) and C (JM403). The standard genome RNAs were detected in the culture supernatants from all MV strains using RT-PCR amplified with primers A and B (Fig. 2*C*, *upper panel*). In contrast, the 5′ copy-back DI RNAs were detected in the culture supernatants of the laboratory adapted strains (NV, ED, and IC-V) and vaccine strains (Schwarz and Tanabe) using RT-PCR amplified with primers A and C (Fig. 2*C*, *lower panel*). The 5′ copy-back DI RNAs were not detected by this method in any wild-type strain or in CAM and AIK-C vaccine strains (Fig. 2*C*, *lower panel*). Amplified fragment sizes of the 5′ copy-back DI RNAs were variable depending on the strains cells were infected with. In Tanabe strains, multiple fragments were detected. These fragments were cloned

Table II. *Properties of DI RNAs of MV strains*

Strains	DI Genome Size (nt)	Stem Size (nt)	Loop (nt)
ED	1152	142	868
NV	726	121	474
ICV	1385	120	1145
Schwarz	1098	177	744
Tanabe[a]	642	103	436
	618	98	422
	474	98	278

[a] At least three patterns were found in 12 clones.

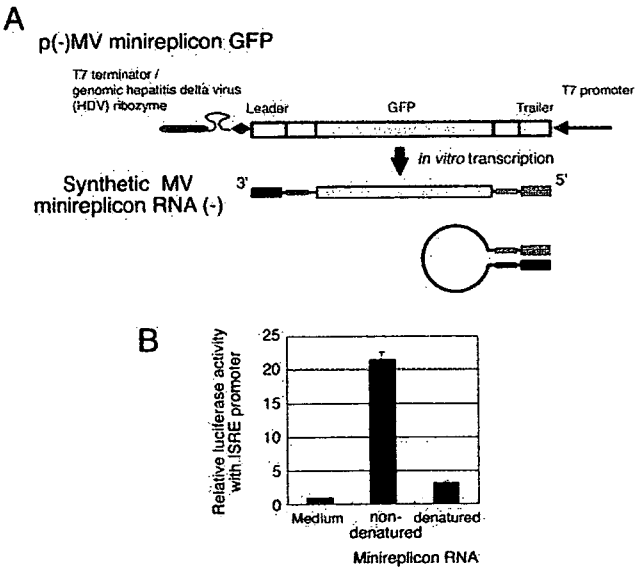

FIGURE 3. Viral minireplicon RNA induces IFN signaling. *A*, Schematic representation of vector p(−)MV minireplicon GFP and transcribed synthetic MV minireplicon GFP RNA$^-$ (linear and stem loop forms). MV minireplicon GFP RNA(−) was transcribed using T7 in vitro transcription. Black boxes and gray boxes were highly complementary to a sequence element, which is present in 3′ and 5′ regions of the MV genome, suggesting that the synthetic MV minireplicon consists of stem and loop. *B*, Synthetic minireplicon RNA activates the ISRE promoter. HEK293 cells were transfected with pISRE-Luc and phRL-TK. Twenty-four hours later, cells were transfected with in vitro-transcribed MV minireplicon RNA, or heat-treated denatured MV minireplicon RNA. Six hours later, the cells were lysed and luciferase reporter assay was performed. The experiments were performed at least three times and a representative one is shown.

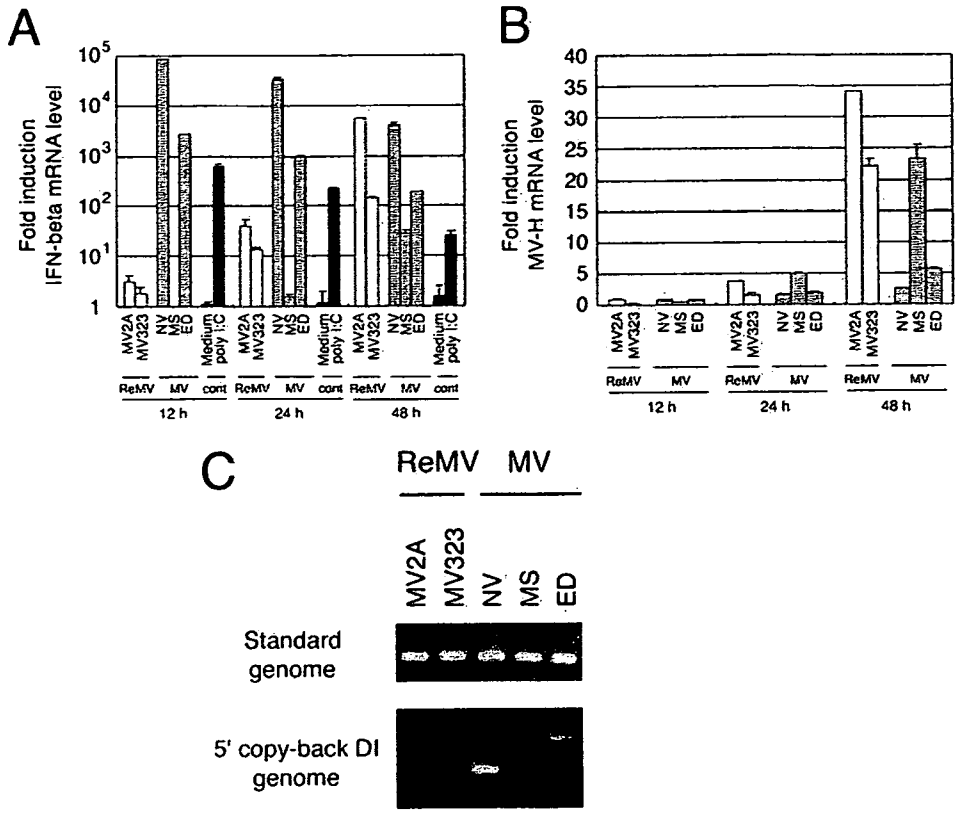

FIGURE 4. MV-containing DI RNA induces robust IFN-β in mDCs in an early phase. IFN-β induction and MV replication profiles in monocyte-derived mDCs. Monocyte-derived mDCs were infected with MV2A (rMV ED strain), MV323 (rMV IC-B strain), NV (laboratory adapted strain with DI RNA), MS (wild-type strain without DI RNA), or ED (laboratory adapted strain with DI RNA) at MOI = 0.1, or treated with medium or poly I:C (20 μg/ml). *A*, Twelve, 24, or 48 h after infection, the mRNA levels of human IFN-β in mDCs infected with each strain were measured by Q-PCR. The values were normalized to that of β-actin mRNA. Fold induction against medium at 12 h is shown. *B*, MV-H mRNA level was also measured by Q-PCR. The value for MV-H mRNA expression was normalized to that of β-actin mRNA. Relative fold induction against infection of each strain at 0 h is shown. Experiments were performed at least three times and representative results are shown. *C*, RT-PCR amplification of 5′ copy-back DI RNA from culture supernatants of rMVs (ReMVs; MV2A and MV323) or MVs (NV, MS, and ED). RT-PCR was performed as described in Fig. 2*C* using standard genome-specific primers (primers A and B, *upper panel*) or DI-specific primers (primers A and C, *lower panel*).

into the plasmid vector and sequenced. Their sizes and predicted structures are shown in Table II and Fig. 2*B*, where the sites of the primers are indicated for detection of DI RNA. Their predicted structures consisted of the stem and loop of various sizes in these DI RNAs (Fig. 2*B*, Table II).

The stem-loop RNA duplex induces IFN-stimulated response element (ISRE) promoter activation

We next examined whether the stem-loop structure of MV is crucial for type I IFN induction. The GFP sequence was inserted into the leader and trailer of MV (Fig. 3*A*). This synthetic RNA (named MV minireplicon RNA) has highly complementary sequence elements in 3′ and 5′ regions (black and gray boxes), which are needed for replication, transcription, and encapsidation. The synthetic MV minireplicon RNA forms the stem-loop containing RNA duplex by these complementary sequences (Fig. 3*A*). IFN-β-inducing activity of MV minireplicon RNA was examined by reporter assay in HEK293 cells. MV minireplicon RNA was either simply added to the cells or transfected by lipofection. When intact MV minireplicon RNA was transfected, luciferase activity with the ISRE promoter showed ~20-fold against that of medium control (Fig. 3*B*). Detectable levels of the ISRE promoter activation were seen only 6 h after the RNA administration (data not shown). Transfection of denatured MV minireplicon RNA resulted in the loss of IFN-inducing function (Fig. 3*B*). Thus, the stem-loop structure rather than the MV-specific RNA sequence may be essential for type I IFN elevated by MV DI RNA.

Measles virus ED strain with 5′ copy-back DI RNA highly induce IFN-β

Because 5′ copy-back DI RNAs forming the stem-loop structures with double helix induce IFN-β, we examined whether type I IFN induction by MV strains correlated with the amplitude of accompanied DI RNA. mDCs were infected with ED strain with DI RNA and rED strain (MV2A) without DI RNA at MOI = 0.1. The mRNA levels of IFN-β and MV-H in mDCs were determined by Q-PCR 12, 24, and 48 h p.i. (Fig. 4*A*). IFN-inducing activity of ED (with DI RNA) was high in an early phase (<12 h) of infection while that of MV2A was low. The IFN-β mRNA levels of cells infected with rMV2A (ED), MV323 (IC), and wild-type MS strain, all lacking DI RNAs, were low at 12 h p.i. and then increased in a time-dependent manner (Fig. 4*A*). Viral growth was monitored with the MV-H mRNA level. MV strains without DI RNAs efficiently replicated in mDCs in comparison with those with DI RNAs (Fig. 4*B*). Presence of DI RNAs in the lots of these MV strains was confirmed using RT-PCR (Fig. 4*C*). Similar results were obtained with A549/CD150 cells (data not shown). Thus, the induction of IFN-β is closely associated with coexisting DI RNAs in an early phase of MV infection.

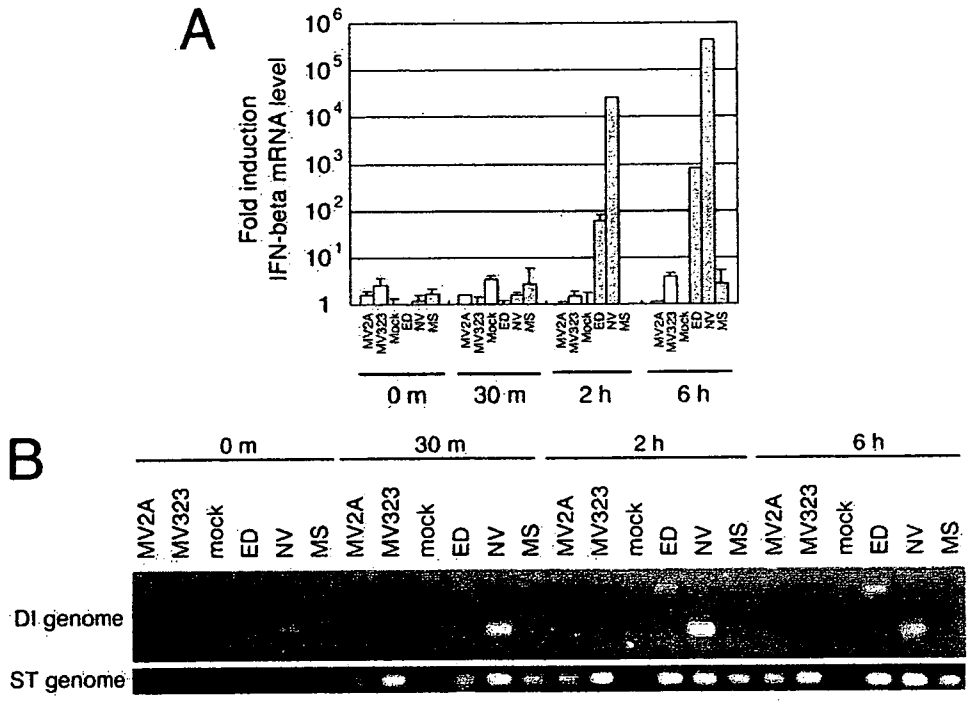

FIGURE 5. MV strain-specific IFN-β mRNA induction in infected cells. *A*, A549/CD150 cells without TLR3 were infected with mock, MV2A (rMV ED strain), MV323 (rMV IC-B strain), NV (laboratory adapted strain with DI RNA), MS (wild-type strain without DI RNA), or ED (laboratory adapted strain with DI RNA) at MOI = 0.1. At timed intervals, RNA samples were recovered and mRNAs of IFN-β and β-actin were measured by Q-PCR. The value for IFN-β mRNA expression was normalized to that of β-actin mRNA. Fold induction against control medium is shown. *B*, RT-PCR for DI RNA and the standard genome of MV was performed as in Fig. 2*C* using genome-specific primers (primers A and B, *upper panel*) or DI-specific primers (primers A and C, *lower panel*). Experiments were performed at least three times and representative results are shown.

In other experiments using A549/CD150 cells, parallelism between the levels of IFN-β mRNA (Fig. 5*A*) and the amplitude of DI RNA (Fig. 5*B*) was analyzed. DI RNA was detected over 30 min, then increased in a time-dependent manner (Fig. 5*B*). Thus, the initial source of DI RNA should be in the virion. Viral DI RNA was increased 2 and 6 h p.i., suggesting that a replication-dependent increase of DI RNA proceeds after the uptake of virion. The IFN induction and the level of DI RNA were almost parallel (Fig. 5, *A* vs *B*).

MV induces IFN via IKKε, TBK-1, and NAK-associated protein 1 (NAP1), but not TICAM-1

mDCs express TLR3 in the endosomes (39) and RIG-I/MDA5 in the cytoplasm (9, 10), which recognize dsRNA. TLR3 recruits TICAM-1/TRIF (29, 40) while RIG-I and MDA5 recruit MAVS/IPS-1/Cardif/VISA adaptors (31, 41–43). They converged upon NAP1, which assembles IKKε and TBK1 to follow the IRF-3-dependnet IFN-β-inducing pathway (28). Gene-silencing analysis was performed to identify the molecules that are involved in MV (ED)-mediated type I IFN induction.

HeLa cells expressing TLR3 responded to poly I:C to induce IFN-β (Fig. 6*A*, *right panel*). The mRNAs of TICAM-1, IKKε, and TBK1 were silenced with siRNA in this study. The gene-silenced cells were infected with MV ED and, 24 h later, the IFN-β mRNA levels were measured with the ED-infected cells. Cells depleted of IKKε or TBK1 hampered the high induction of IFN-β mRNA (Fig. 6*A*, *left panel*), suggesting that the two kinases are crucial factors for IFN-β induction. In contrast, the absence of TICAM-1 barely affected the ED-derived IFN-β mRNA level (Fig. 6*A*, *left panel*). Cells stimulated with poly I:C were used as control for the TLR3 pathway and, as expected, poly I:C-dependent IFN-β induction depended on TICAM-1, IKKε, and TBK1 (Fig. 6*A*, *right panel*). Likewise, NAP1 knockdown exhibited down-regulation of the IFN-β mRNA (Fig. 6*B*) when cells with stably silenced NAP1 or GFP were used instead of the transient knockdown cells (28). When NAP1-depleted cells were stimulated with poly I:C, 40% of the mRNA level was reduced within 6 h (cells die during long-term incubation with poly I:C). In the HeLa cell system, ED infection resulted in a 50% decrease of the NAP1-associated IFN-β induction. The incomplete blockade of IFN-β induction by NAP1 silencing may reflect the presence of an escaping NAP1 moiety due to a high endogenous level of NAP1 or functional compensation of NAP1 with other TANK family proteins (28, 44). Thus, MV ED induces IFN-β in HeLa cells, which involves NAP1, IKKε, and TBK1, but not TICAM-1. Therefore, the trigger for type I IFN induction by DI RNA is not the TLR3-TICAM-1 pathway.

Both RIG-I and MDA5 sense DI RNA

To determine whether RIG-I and/or MDA5 recognize DI RNA, we transfected the MV minireplicon RNA into HEK293/pISRE-luc cells (Fig. 3*B*) subtly overexpressing RIG-I or MDA5. ISRE promoter activation was 12-~18-fold increased due to the minimal constitutive expression of RIG-1or MDA5 (*left control bars* in Fig. 7). When DI RNA was added into the cytoplasm, high ISRE promoter activation was induced in these cells (Fig. 7). DI RNA was heated to denature the stem-loop structure or treated with CIAP to remove 5′ phosphates. In RIG-I-expressing cells, CIAP treatment of DI RNA more significantly reduced RIG-I-mediated IFN promoter activation than heat denaturation. In contrast, the reverse is true in MDA5-expressing cells, where CIAP treatment had almost no effect on MDA5-mediated IFN promoter activation. Hence, DI RNA enhances both RIG-I- and MDA5-mediated IFN-β induction. Both sense the stem-loop structure, while only RIG-I senses 5′ phosphates under the conditions setting.

DI RNA stimulates the cytoplasmic IFN-inducing pathway

We finally examined whether DI RNAs of MV follows the pathway involving RIG-I/MDA5 and MAVS for signaling IFN-β induction by gene-silencing technology. RIG-I, MDA5, MAVS, and TICAM-1 were silenced with siRNA (Fig. 8*A*), then MV minireplicon RNA or poly I:C was transfected into HeLa cells. Six hours later, the IFN-β mRNA levels were measured by Q-PCR (Fig. 8*B*). The siRNA of GFP was used as control. When MV minireplicon RNA was transfected into HeLa cells, the IFN-β mRNA levels in

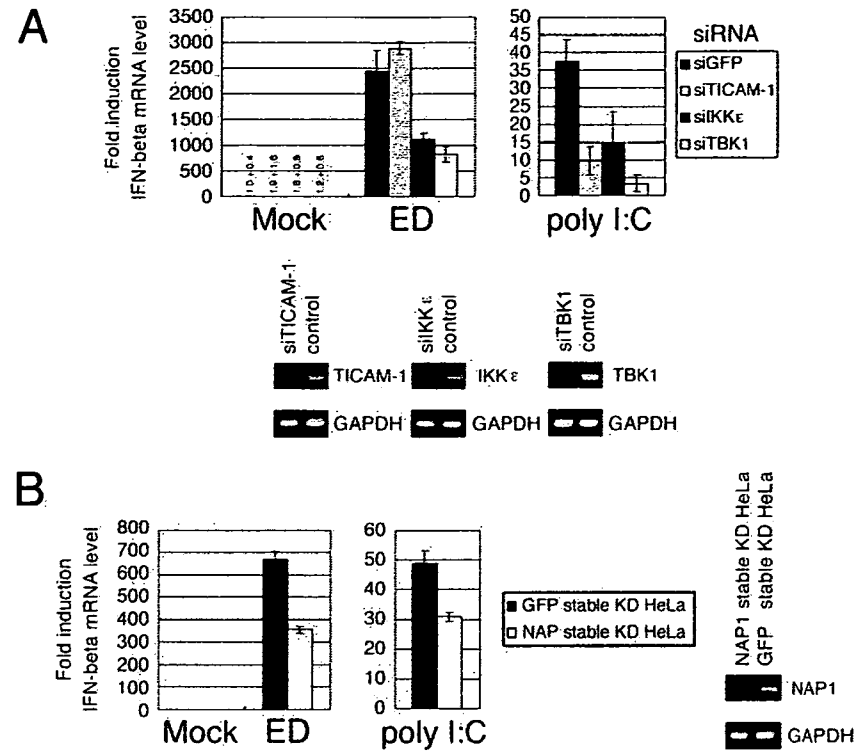

FIGURE 6. MV ED-mediated type I IFN induction depends on IKKε, TBK1, and NAP1, but not on TICAM-1. *A*, HeLa cells with TLR3 were transfected with siRNA targeted at TICAM-1, IKKε, or TBK1, and 72 h later cells were treated with Mock, ED, or poly I:C. Twenty-four hours later, RNA samples were recovered and mRNAs of IFN-β and β-actin were measured using RT- and Q-PCR. Normalization was performed. Relative fold induction against mock infection in GFP knockdown is shown. *B*, NAP1 or GFP stable knockdown HeLa cells were treated with Mock, ED (24 h), or poly I:C (2 h), and Q-PCR was performed as in *A*. Knockdown of each mRNA was confirmed by RT-PCR. Experiments were performed at least three times and representative results are shown.

the RIG-I- or MAVS-silenced cells were decreased by <20% of the control GFP siRNA cells. In the MDA5- or TBK1-silenced cells, the IFN-β mRNA levels were decreased by >50% of the control. In TICAM-1 silencing, however, no decrease of IFN-β mRNA was observed. When poly I:C was transfected, the cells efficiently induced IFN-β. The level of IFN-β mRNA was decreased in cells depleted of MDA5, MAVS, or TBK1 to ~25% of the GFP control (Fig. 8*B*). RIG-I silencing resulted in a 40% decrease of IFN-β induction in this setting. TICAM-1 silencing minimally affected the IFN-β mRNA level, suggesting that participation of TLR3 in IFN-β induction is negligible in HeLa cells. Taken together, these results strongly suggest that DI RNA induces IFN-β through the RIG-I/MDA5-MAVS pathway in the cytoplasm.

Similar experiments were performed using HeLa cells depleted of the factors in the IFN-inducing pathways and various MV strains. The rMV2A induced >100-fold less amounts of IFN-β mRNA compared with MV minireplicon RNA under the same conditions. ED and NV strains having DI RNA efficiently induced IFN-β mRNA early in infection of HeLa cells (Fig. 8*C*, *right panel*). The minute induction of IFN-β was suppressed by knockdown of RIG-I or MDA5 while MAVS silencing resulted in complete abrogation of IFN-β induction (Fig. 8*C*, *left panel*). Hence, in HeLa cells RIG-I and MDA5 share the IFN-β-inducing ability which totally relies on MAVS. Thus, the results again support the importance of DI RNA in IFN-β induction and involvement of the cytoplasmic RIG-I pathway in the induction of IFN-β in MV infection.

Discussion

MV is a negative-strand RNA virus which is believed to generate dsRNA for virus replication. However, a recent report suggested that influenza virus barely produces more than the detection limit

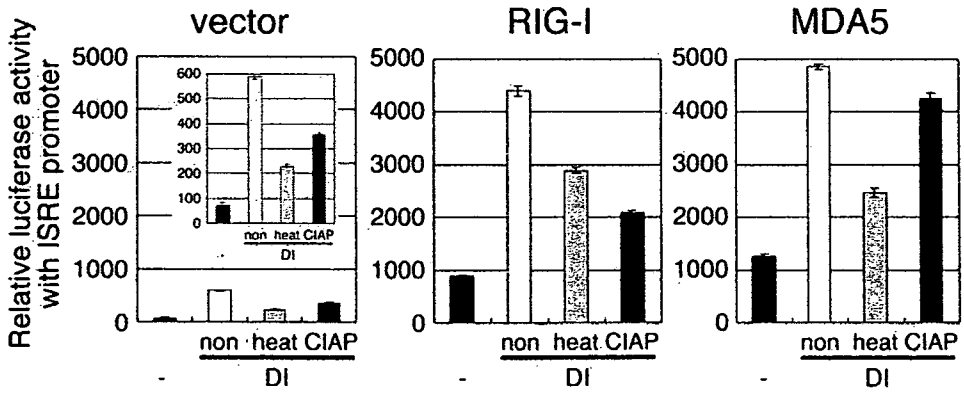

FIGURE 7. Phosphorylation and duplex structure of DI RNA differentially contribute to ISRE promoter activation via the cytoplasmic RNA sensors. HEK293 cells with pISRE-luc were prepared as in Fig. 3*B*. HEK cells were transfected with full-length RIG-I (*center panel*) or MDA5 (200 μg/5 × 10^5 cells; *right panel*) by polyfection. Empty vector was used as a control (*left panel*). Twenty-four hours later, cells were transfected with GFP minireplicon RNA (8 μg/ml) by Lipofectamine 2000. Six hours later, cells were harvested for reporter assay. Closed bars to the *left* in each panel represent reporter activity of cells with no stimuli, whereas DI means loading DI RNA. Non, Intact DI RNA; heat, heat-inactivated DI RNA; CIAP, CIAP-treated DI RNA. One of two similar experiments is shown.

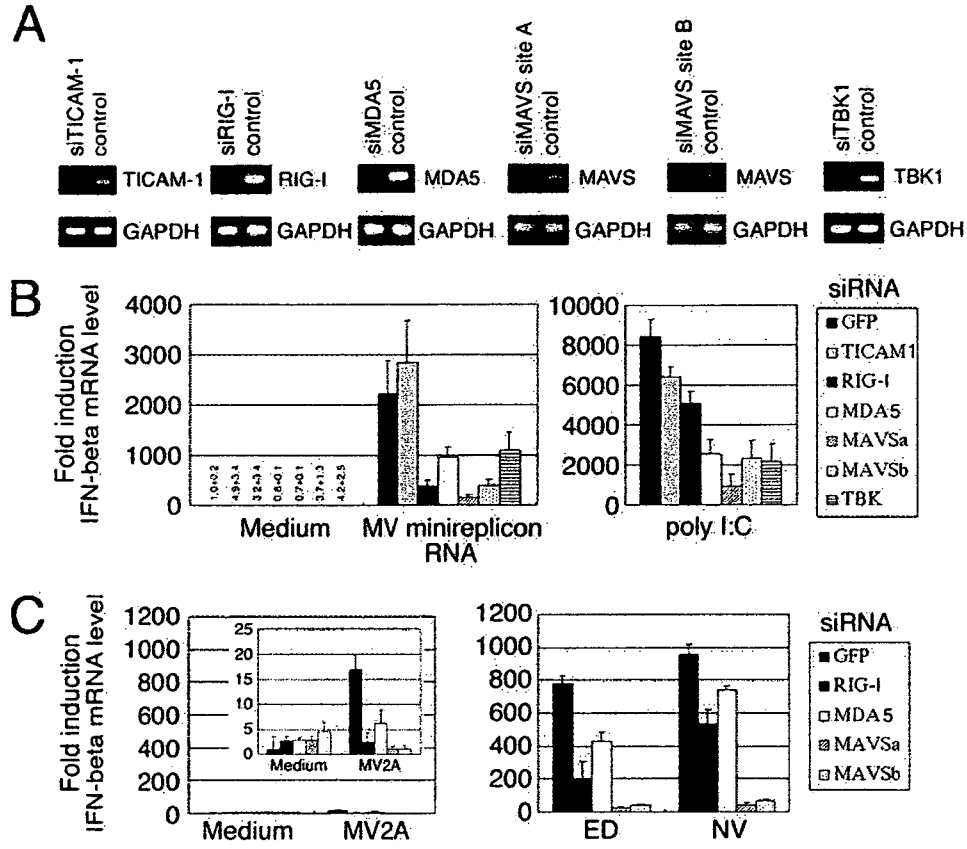

FIGURE 8. The route for type I IFN induction by MV minireplicon RNA and MV strains. HeLa cells were transfected with siRNA targeted at TICAM-1, RIG-I, MDA5, MAVS site A and B, or TBK1. *A*, Knockdown of each mRNA was confirmed by RT-PCR. *B*, Seventy-two hours after siRNA transfection, cells were transfected with MV minireplicon or poly I:C; or *C*, treated with Mock, MV2A (rMV ED strain), ED, or NV (ED and NV were laboratory adapted strains with 5′ copy-back DI). Twenty-four hours later, RNA samples were recovered and the mRNA levels of IFN-β, and β-actin were measured using RT- and Q-PCR. Normalization was performed. Relative fold induction against medium or mock infection in GFP knockdown is shown. The experiments were performed at least three times and representative results are shown.

of dsRNA by quantitative ELISA (45). Instead, triphosphate ssRNA activates RIG-I and induces IFN-α/IFN-β (45, 46). What is responsible for IFN induction in MV-infected cells has remained largely unknown. Here, we demonstrated that DI RNA participates in MV-mediated IRF-3 activation and type I IFN induction, which occur before virus replication (early phase). Infection with wild-type MV would produce triphosphate ssRNA but in the amount less than that required to activate RIG-I.

Naniche et al. and we previously reported that wild-type MV strains barely produce type I IFN during infection (16, 21). We demonstrated that an early induction of type I IFN by vaccine and laboratory adapted strains of MV depends on the coincidental DI RNA that resides in the virus particles. DI RNA rapidly induced type I IFNs, usually within 2 h after the virion fused with host cells. In contrast, effective viral RNA replication started 12 h p.i. Thus, in the context of DI RNA, IFN induction precedes viral replication to prevent the host cells from damage that accompanies viral replication. Furthermore, replication of the viral genome is retarded once DI RNA replicates in the same cells. At least, MV DI RNA inhibits viral amplification by two independent ways: IRF-3-mediated type I IFN induction and blockage of viral replication. Ultimately, virus strains containing DI RNA are attenuated in host cells by multiple means. Vaccine and laboratory adapted strains tend to possess DI RNA in addition to the genome within the particle. This DI RNA may act as a suppressor of virulence for initial step of virus infection.

We have learned from an earlier study on the MV substrains IC-B (84-01 B95a isolate) and IC-V (84-01 Vero isolate) (22) that the MV isolates from a single patient with acute measles gave rise to differential contents of DI RNA. The B95a-propagated substrain (IC-B) was highly pathogenic in experimental infection with cynomolgus monkeys while the Vero-propagated substrain (IC-V) had low pathogenicity in vivo. We have carefully propagated the MV strains IC-V and IC-B from their original lots and reproducibly detected DI RNA in the IC-V but not the IC-B stock. The MV substrains IC-B and IC-V derived from the same clinical material behave like wild-type and laboratory adapted strains, respectively. Their differential infectious properties appear to be rooted in the properties of the cells where the viruses were propagated. B95a cells can take up broad viral populations through the two orthologs of CD46 and CD150. Vero cells are known to have some deficiency in IFN induction (47). Adaptation of MV strains to Vero cells may foster amplification of DI RNA leading to the formation of DI RNA-containing virus particles that possess less toxicity by inducing type I IFN and blocking replication.

We performed PCR assay using the several original lots of the vaccine strains to detect the DI RNA. Unexpectedly, DI RNA was not detected in the CAM and AIK-C vaccine strains at least at the conditions used. It is possible that these two strains actually do not contain DI RNA or the primers chosen do not recognize the putative DI RNA sequences of these strains. As CAM and AIK-C have been established via plaque purification (48, 49), the original plaque may not have contained DI RNA. Alternatively, V or C proteins of these vaccine strains may be less functional for inhibition of IFNR-mediated amplification of type I IFN production (38, 50). The actual mechanism by which type I IFN is induced in CAM- or AIK-C-infected cells needs further investigation.

Previous studies suggested that the MV N-protein acts as a type I IFN inducer (36, 37). We found that N-protein minimally enhances IFN-α/IFN-β production and in conjunction with DI RNA far more up-regulates the IFN production than N protein alone (data not shown). Although the mechanism by which N protein potentiates DI RNA-mediated IFN production in the cells expressing the minireplicon RNA is intriguing, the possibility of interaction between the N protein and DI RNA has remained unaddressed. Anyhow, DI RNA rather than N protein is a potential

factor affecting the degree of IFN-α/IFN-β induction in the infected cells.

IFN-β was induced in human cells expressing either CD46 or CD150 in response to the infection by laboratory adapted strains. Laboratory and vaccine strains use CD46 in addition to CD150 as an entry receptor (51, 52). Wild-type strains do not enter the cells via CD46 (17, 18). As CD46 is ubiquitously expressed in human cells, including lymphocytes, mDCs, and macrophages, one can predict that CD46 is associated with IFN-β-inducing signals (53). However, irrespective of several experimental trials, we could not connect CD46 signaling with IFN-β induction (54). One possibility is that DI RNA production inadvertently coincides with CD46 receptor usage during MV strains passage in Vero cells. Recent reports indicate that CD46 functions as an immune modulator in lymphocytes and dendritic cells/macrophages (55, 56). The possibility that CD46 is involved in DI RNA-mediated immune responses should be revisited. Likewise, further studies on the properties of the RNA polymerase, nucleocapsid, and MV V protein in association with DI RNA production and receptor signal output in MV-infected cells will be required for further elucidation of measles-mediated immune modulation.

Previous reports suggested that the production of DI RNA is associated with viral-persistent infection (34). We considered whether DI RNA has an ability to regulate MV-persistent infection. DI RNA suppresses viral replication and reciprocally accelerates host IFN induction. Under the conditions where DI RNAs are being produced in cells, viruses are difficult to proliferate. Virus must change and adapt to the hostile environment for its survival and persistency of infection. Thus, DI RNA may be a factor to promote virus evolution and selective adaptation of viruses to host cells. However, the question still remains as to what factor is responsible for promoting initial viral persistency. If DI RNA plays a pivotal role in advancing viral adaptation, one could envisage it as a two-edged sword, decreasing pathogenicity and enhancing persistent infection. Additional study is needed to further explore this possibility.

After completing this study, we found two articles that were released relating to Sendai virus (SeV) DI RNA (57, 58). The level of IFN-β activation is shown to be proportional to that of SeV DI RNA replication and the viral V and C proteins are effective in blocking the copy-back DI RNA-induced activation of the IFN-β promoter (57). The other investigators state that SeV DI RNA is required for its robust mDC maturation (58). These investigators claim the importance of RIG-I in DI RNA-mediated IFN-β induction in SeV. In this study, we not only experimentally show that DI RNA activates IRF-3, but also further define the pathway taken by DI RNA to produce robust IFN-β. In MV ED studies, DI RNA, rather than the formation of the genomic dsRNA, causes IFN-β induction and mDC maturation in infected cells.

Note added in proof. Importance of 5′-phosphate-ended RNA in activation of RIG-I-mediated IFN response was also reported in MV infection by Plumet et al. (59).

Acknowledgments

We are grateful to Drs. A. Hirano (University of Washington, Seattle, WA), Y. Yanagi (Kyushu University, Hakata, Japan), F. Kobune (National Institutes of Health, Tokyo, Japan), T. Kimoto (Osaka Prefectural Public Health Institute, Osaka, Japan), A. Ueda (Osaka University, Osaka, Japan), K. Takeuchi (Tsukuba University, Ibaraki, Japan), N. Inoue, T. Akazawa (Osaka Medical Center for Cancer, Osaka, Japan), and M. Ayata (Osaka City University, Osaka, Japan) for providing cells, MV strains, and discussions. Thanks are also due to M. Kurita-Taniguchi (Osaka Medical Center for Cancer, Osaka, Japan) for technical assistance.

Disclosures

The authors have no financial conflict of interest.

References

1. Honda, K., A. Takaoka, and T. Taniguchi. 2006. Type I interferon gene induction by the interferon regulatory factor family of transcription factors. *Immunity* 25: 349–360.
2. Fitzgerald, K. A. 2006. Viral targeting of interferon regulatory factor-3 and type I interferon gene transcription. *Future Virol.* 1: 783–793.
3. Alexopoulou, L., A. C. Holt, R. Medzhitov, and R. A. Flavell. 2001. Recognition of double-stranded RNA and activation of NF-κB by Toll-like receptor 3. *Nature* 413: 732–738.
4. Matsumoto, M., S. Kikkawa, M. Kohase, K. Miyake, and T. Seya. 2002. Establishment of a monoclonal antibody against human Toll-like receptor 3 that blocks double-stranded RNA-mediated signaling. *Biochem. Biophys. Res. Commun.* 293: 1364–1369.
5. Heil, F., H. Hemmi, H. Hochrein, F. Ampenberger, C. Kirschning, S. Akira, G. Lipford, H. Wagner, and S. Bauer. 2004. Species-specific recognition of single-stranded RNA via Toll-like receptor 7 and 8. *Science* 303: 1526–1529.
6. Diebold, S. S., T. Kaisho, H. Hemmi, S. Akira, and C. Reis e Sousa. 2004. Innate antiviral responses by means of TLR7-mediated recognition of single-stranded RNA. *Science* 303: 1529–1531.
7. Hemmi, H., O. Takeuchi, T. Kawai, T. Kaisho, S. Sato, H. Sanjo, M. Matsumoto, K. Hoshino, H. Wagner, K. Takeda, and S. Akira. 2000. A Toll-like receptor recognizes bacterial DNA. *Nature* 408: 740–745.
8. Yang, Y. L., L. F. Reis, J. Pavlovic, A. Aguzzi, R. Schafer, A. Kumar, B. R. Williams, M. Aguet, and C. Weissmann. 1995. Deficient signaling in mice devoid of double-stranded RNA-dependent protein kinase. *EMBO J.* 14: 6095–6106.
9. Yoneyama, M., M. Kikuchi, T. Natsukawa, N. Shinobu, T. Imaizumi, M. Miyagishi, K. Taira, S. Akira, and T. Fujita. 2004. The RNA helicase RIG-I has an essential function in double-stranded RNA-induced innate antiviral responses. *Nat. Immunol.* 5: 730–737.
10. Andrejeva, J., K. S. Childs, D. F. Young, T. S. Carlos, N. Stock, S. Goodbourn, and R. E. Randall. 2004. The V proteins of paramyxoviruses bind the IFN-inducible RNA helicase, mda-5, and inhibit its activation of the IFN-β promoter. *Proc. Natl. Acad. Sci. USA* 101: 17264–17269.
11. Akazawa, T., T. Ebihara, M. Okuno, Y. Okuda, M. Shingai, K. Tsujimura, T. Takahashi, M. Ikawa, M. Okabe, N. Inoue, et al. 2007. Antitumor NK activation induced by the Toll-like receptor 3-TICAM-1 (TRIF) pathway in myeloid dendritic cells. *Proc. Natl. Acad. Sci. USA* 104: 252–257.
12. Biron, C. A., and L. Brossay. 2001. NK cells and NKT cells in innate defense against viral infections. *Curr. Opin. Immunol.* 13: 458–464.
13. Freigang, S., H. C. Probst, and M. van den Broek. 2005. DC infection promotes antiviral CTL priming: the "Winkelried" strategy. *Trends Immunol.* 26: 13–18.
14. Gotoh, B., T. Komatsu, K. Takeuchi, and J. Yokoo. 2002. Paramyxovirus strategies for evading the interferon response. *Rev. Med. Virol.* 12: 337–357.
15. Hengel, H., U. H. Koszinowski, and K. K. Conzelmann. 2005. Viruses know it all: new insights into IFN networks. *Trends Immunol.* 26: 396–401.
16. Naniche, D., A. Yeh, D. Eto, M. Manchester, R. M. Friedman, and M. B. A. Oldstone. 2000. Evasion of host defenses by measles virus: wild-type measles virus infection interferes with induction of α/β interferon production. *J. Virol.* 74: 7478–7484.
17. Lazzarini, R. A., J. D. Keene, and M. Schubert. 1981. The origins of defective interfering particles of the negative-strand RNA viruses. *Cell* 26: 145–154.
18. Tatsuo, H., N. Ono, K. Tanaka, and Y. Yanagi. 2000. SLAM (CDw150) is a cellular receptor for measles virus. *Nature* 406: 893–897.
19. Ono, N., H. Tatsuo, Y. Hidaka, T. Aoki, H. Minagawa, and Y. Yanagi. 2001. Measles viruses on throat swabs from measles patients use signaling lymphocytic activation molecule (CDw150) but not CD46 as a cellular receptor. *J. Virol.* 75: 4399–4401.
20. Seya, T., T. Hara, M. Matsumoto, and H. Akedo. 1990. Quantitative analysis of membrane cofactor protein (MCP) of complement: High expression of MCP on human leukemia cell lines, which is down-regulated during cell-differentiation. *J. Immunol.* 145: 238–245.
21. Murabayashi, N., M. Kurita-Taniguchi, M. Ayata, M. Matsumoto, H. Ogura, and T. Seya. 2002. Susceptibility of human dendritic cells (DCs) to measles virus (MV) depends on their activation stages in conjunction with the level of CDw150: role of Toll stimulators in DC maturation and MV amplification. *Microbes Infect.* 4: 785–794.
22. Kobune, F., H. Sakata, and A. Sugiura. 1990. Marmoset lymphoblastoid cells as a sensitive host for isolation of measles virus. *J. Virol.* 64: 700–705.
23. Ayata, M., T. Kimoto, K. Hayashi, T. Seto, R. Murata, and H. Ogura. 1998. Nucleotide sequences of the matrix protein gene of subacute sclerosing panencephalitis viruses compared with local contemporary isolates from patients with acute measles. *Virus Res.* 54: 107–115.
24. Kurita-Taniguchi, M., A. Fukui, K. Hazeki, A. Hirano, S. Tsuji, M. Matsumoto, M. Watanabe, S. Ueda, and T. Seya. 2000. Functional modulation of human macrophages through CD46 (measles virus receptor): production of IL-12 p40 and nitric oxide in association with recruitment of protein-tyrosine phosphatase SHP-1 to CD46. *J. Immunol.* 165: 5143–5152.
25. Kurita-Taniguchi, M., K. Hazeki, N. Murabayashi, A. Fukui, S. Tsuji, M. Matsumoto, K. Toyoshima, and T. Seya. 2002. Molecular assembly of CD46 with CD9, α_3-β_1 integrin and protein tyrosine phosphatase SHP-1 in human macrophages through differentiation by GM-CSF. *Mol. Immunol.* 38: 689–700.

26. Nishiguchi, M., M. Matsumoto, T. Takao, M. Hoshino, Y. Shimonishi, S. Tsuji, N. A. Begum, O. Takeuchi, S. Akira, K. Toyoshima, and T. Seya. 2001. Mycoplasma fermentans lipoprotein M161Ag-induced cell activation is mediated by Toll-like receptor 2: role of N-terminal hydrophobic portion in its multiple functions. *J. Immunol.* 166: 2610–2616.
27. Shingai, M., N. Inoue, T. Okuno, M. Okabe, T. Akazawa, Y. Miyamoto, M. Ayata, K. Honda, M. Kurita-Taniguchi, M. Matsumoto, et al. 2005. Wild-type measles virus infection in human CD46/CD150-transgenic mice: CD11c-positive dendritic cells establish systemic viral infection. *J. Immunol.* 175: 3252–3261.
28. Sasai, M., M. Shingai, K. Funami, M. Yoneyama, T. Fujita, M. Matsumoto, and T. Seya. 2006. NAK-assiciated protein 1 participates in both the TLR3 and the cytoplasmic pathways in type I IFN induction. *J. Immunol.* 177: 8676–8683.
29. Oshiumi, H., M. Matsumoto, K. Funami, T. Akazawa, and T. Seya. 2003. TICAM-1, an adaptor molecule that participates in Toll-like receptor 3-mediated interferon-β induction. *Nat. Immunol.* 4: 161–167.
30. Fitzgerald, K. A., S. M. McWhirter, K. L. Faia, D. C. Rowe, E. Latz, D. T. Golenbock, A. J. Coyle, S. M. Liao, and T. Maniatis. 2003. IKKε and TBK1 are essential components of the IRF3 signaling pathway. *Nat. Inunnol.* 4: 491–496.
31. Seth, R. B., L. Sun, C. K. Ea, and Z. J. Chen. 2005. Identification and characterization of MAVS, a mitochondrial antiviral signaling protein that activates NF-κB and IRF 3. *Cell* 122: 669–682.
32. Takeda, M., K. Takeuchi, N. Miyajima, F. Kobune, Y. Ami, N. Nagata, Y. Suzaki, Y. Nagai, and M. Tashiro. 2000. Recovery of pathogenic measles virus from cloned cDNA. *J. Virol.* 74: 6643–6647.
33. Calain, P., J. Curran, D. Kolakofsky, and L. Roux. 1992. Molecular cloning of natural paramyxovirus copy-back defective interfering RNAs and their expression from DNA. *Virology* 191: 62–71.
34. Sidhu, M. S., J. Crowley, A. Lowenthal, D. Karcher, J. Menonna, S. Cook, S. Udem, and P. Dowling. 1994. Defective measles virus in human subacute sclerosing panencephalitis brain. *Virology* 202: 631–641.
35. Whistler, T., W. J. Bellini, and P. A. Rota. 1996. Generation of defective interfering particles by two vaccine strains of measles virus. *Virology* 220: 480–484.
36. Sharma, S., B. R. tenOever, N. Grandvaux, G. P. Zhou, R. Lin, and J. Hiscott. 2003. Triggering the interferon antiviral response through an IKK-related pathway. *Science* 300: 1148–1151.
37. tenOever, B. R., M. J. Servant, N. Grandvaux, R. Lin, and J. Hiscott. 2002. Recognition of the measles virus nucleocapsid as a mechanism of IRF-3 activation. *J. Virol.* 76: 3659–3669.
38. Takeuchi, K., S. I. Kadota, M. Takeda, N. Miyajima, and K. Nagata. 2003. Measles virus V protein blocks interferon (IFN)-α/β but not IFN-γ signaling by inhibiting STAT1 and STAT2 phosphorylation. *FEBS Lett.* 545: 177–182.
39. Matsumoto, M., K. Funami, M. Tanabe, H. Oshiumi, M. Shingai, Y. Seto, A. Yamamoto, and T. Seya. 2003. Subcellular localization of Toll-like receptor 3 in human dendritic cells. *J. Immunol.* 171: 3154–3162.
40. Yamamoto, M., S. Sato, K. Mori, K. Hoshino, O. Takeuchi, K. Takeda, and S. Akira. 2002. Cutting edge: a novel Toll/IL-1 receptor domain-containing adapter that preferentially activates the IFN-β promoter in the Toll-like receptor signaling. *J. Inunnol.* 169: 6668–6672.
41. Meylan, E., J. Curran, K. Hofmann, D. Moradpour, M. Binder, R. Bartenschlager, and J. Tschopp. 2005. Cardif is an adaptor protein in the RIG-I antiviral pathway and is targeted by hepatitis C virus. *Nature* 437: 1167–1172.
42. Kawai, T., K. Takahashi, S. Sato, C. Coban, H. Kumar, H. Kato, K. J. Ishii, O. Takeuchi, and S. Akira. 2005. IPS-1, an adaptor triggering RIG-I- and Mda5-mediated type I interferon induction. *Nat. Immunol.* 6: 981–988.
43. Xu, L. G., Y. Y. Wang, K. J. Han, L. Y. Li, Z. Zhai, and H. B. Shu. 2005. VISA is an adapter protein required for virus-triggered IFN-β signaling. *Mol. Cell* 19: 727–740.
44. Sasai, M., M. Matsumoto, and T. Seya. 2006. The kinase complex responsible for IRF-3-mediated IFN-β production in myeloid dendritic cells (mDC). *J. Biochem.* 139: 171–175.
45. Hornung, V., J. Ellegast, S. Kim, K. Brzozka, A. Jung, H. Kato, H. Poeck, S. Akira, K. K. Conzelmann, M. Schlee, et al. 2006. 5′-Triphosphate RNA is the ligand for RIG-I. *Science* 314: 994–997.
46. Pichlmair, A., O. Schulz, C. P. Tan, T. I. Naslund, P. Liljestrom, F. Weber, and C. Reis e Sousa. 2006. RIG-I-mediated antiviral responses to single-stranded RNA bearing 5′-phosphates. *Science* 314: 997–1001.
47. Mosca, J. D., and P. M. Pitha. 1986. Transcriptional and posttranscriptional regulation of exogenous human β interferon gene in simian cells defective in interferon synthesis. *Mol. Cell. Biol.* 6: 2279–2283.
48. Makino, S., K. Sasaki, N. Nakamura, M. Nakagawa, and S. Nakajima. 1974. Studies on the modification of the live AIK measles vaccine. II. Development and evaluation of the live AIK-C measles vaccine. *Kitasato Arch. Exp. Med.* 47: 13–21.
49. Takaku, K., T. Sasada, T. Konobe, K. Onishi, and S. Ueda. 1970. Studies on further attenuated live measles vaccine. 3. Selection of less reactive variants of CAM measles vaccine virus. *Biken J.* 13: 163–168.
50. Nakatsu, Y., M. Takeda, S. Ohno, R. Koga, and Y. Yanagi. 2006. Translational inhibition and increased interferon induction in cells infected with C protein-deficient measles virus. *J. Virol.* 80: 11861–11867.
51. Yanagi, Y., M. Takeda, and S. Ohno. 2006. Measles virus: cellular receptors, tropism and pathogenesis. *J. Gen. Virol.* 87: 2767–2779.
52. Oldstone, M. B. A., D. Homann, H. Lewicki, and D. Stevenson. 2002. One, two, or three step: measles virus receptor dance. *Virology* 299: 162–163.
53. Katayama, Y., A. Hirano, and T. C. Wong. 2000. Human receptor for measles virus (CD46) enhances nitric oxide production and restricts virus replication in mouse macrophages by modulating production of α/β interferon. *J. Virol.* 74: 1252–1257.
54. Hirano, A., M. Kurita-Taniguchi, Y. Katayama, M. Matsumoto, T. C. Wong, and T. Seya. 2002. Isoform-specific ligation of human CD46 enhances interferon γ-dependent nitric oxide production in macrophages. *J. Biochem.* 132: 83–91.
55. Kemper, C., J. W. Verbsky, J. D. Price, and J. P. Atkinson. 2005. T-cell stimulation and regulation: with complements from CD46. *Immunol. Res.* 32: 31–43.
56. Oliaro, J., A. Pasam, N. J. Waterhouse, K. A. Browne, M. J. Ludford-Menting, J. A. Trapani, and S. M. Russell. 2006. Ligation of the cell surface receptor, CD46, alters T cell polarity and response to antigen presentation. *Proc. Natl. Acad. Sci. USA* 103: 18685–18690.
57. Strahle, L., D. Garcin, and D. Kolakofsky. 2006. Sendai virus defective-interfering genomes and the activation of interferon-β. *Virology* 351: 101–111.
58. Yount, J. S., T. A. Kraus, C. M. Horvath, T. M. Moran, and C. B. Lopez. 2006. A novel role for viral-defective interfering particles in enhancing dendritic cell maturation. *J. Immunol.* 177: 4503–4513.
59. Plumet, S., F. Herschke, J. M. Bourhis, H. Valentin, S. Longhi, and D. Gerlier. 2007. Cytosolic 5′-triphosphate ended viral leader transcript of measles virus as activator of the RIG-I-mediated interferon response. *PloS ONE* 2: e279.

«paper no. vir83510 charlesworth ref: vir83510»

Animal RNA

Journal of General Virology (2008), 89, 000–000 DOI 10.1099/vir.0.83510-0

Hepatitis C virus NS5A protein interacts with and negatively regulates the non-receptor protein tyrosine kinase Syk

Sachiko Inubushi,[1]† Motoko Nagano-Fujii,[1]† Kikumi Kitayama,[1] Motofumi Tanaka,[1] Chunying An,[1] Hiroshi Yokozaki,[2] Hirohei Yamamura,[3] Hideko Nuriya,[4] Michinori Kohara,[4] Kiyonao Sada[1]‡ and Hak Hotta[1]

Correspondence
Hak Hotta
hotta@kobe-u.ac.jp

[1]Division of Microbiology, Kobe University Graduate School of Medicine, Kobe 650-0017, Japan

[2]Division of Surgical Pathology, Kobe University Graduate School of Medicine, Kobe 650-0017, Japan

[3]Hyogo Laboratory, Hyogo Prefectural Institute of Public Health and Environmental Sciences, Kobe 652-0032, Japan

[4]Department of Microbiology and Cell Biology, The Tokyo Metropolitan Institute of Medical Science, Tokyo 113-8613, Japan

Hepatitis C virus (HCV) is the major causative agent of hepatocellular carcinoma. However, the precise mechanism underlying the carcinogenesis is yet to be elucidated. It has recently been reported that Syk, a non-receptor protein tyrosine kinase, functions as a potent tumour suppressor in human breast carcinoma. This study first examined the possible effect of HCV infection on expression of Syk *in vivo*. Immunohistochemical analysis revealed that endogenous Syk, which otherwise was expressed diffusely in the cytoplasm of normal hepatocytes, was localized near the cell membrane with a patchy pattern in HCV-infected hepatocytes. The possible interaction between HCV proteins and Syk in human hepatoma-derived Huh-7 cells was then examined. Immunoprecipitation analysis revealed that NS5A interacted strongly with Syk. Deletion-mutation analysis revealed that an N-terminal portion of NS5A (aa 1–175) was involved in the physical interaction with Syk. An *in vitro* kinase assay demonstrated that NS5A inhibited the enzymic activity of Syk and that, in addition to the N-terminal 175 residues, a central portion of NS5A (aa 237–302) was required for inhibition of Syk. Moreover, Syk-mediated phosphorylation of phospholipase C-γ1 was downregulated by NS5A. An interaction of NS5A with Syk was also detected in Huh-7.5 cells harbouring an HCV RNA replicon or infected with HCV. In conclusion, these results demonstrated that NS5A interacts with Syk resulting in negative regulation of its kinase activity. The results indicate that that NS5A may be involved in the carcinogenesis of hepatocytes through the suppression of Syk kinase activities.

Received 11 October 2007
Accepted 14 January 2008

INTRODUCTION

Hepatitis C virus (HCV) is the major aetiological agent of viral hepatitis worldwide after hepatitis A and B viruses (Choo *et al.*, 1989), with about 170 million people being infected. The majority of HCV-infected individuals develop chronic infection, which may progress to liver cirrhosis and hepatocellular carcinoma (HCC). HCV is a member of the family *Flaviviridae* and its genome consists of a single-stranded, positive-sense RNA of approximately 9600 nt, which encodes a polyprotein precursor of about 3010 aa. Currently, clinical HCV isolates are classified into six genotypes and more than 60 subtypes (Doi *et al.*, 1996; Mellor *et al.*, 1995; Robertson *et al.*, 1998). The polyprotein is cleaved by signal peptidase, signal peptide peptidase and two virally encoded proteases to generate at least ten mature proteins: core, envelope glycoprotein 1 (E1), E2, p7, non-structural protein 2 (NS2), NS3, NS4A, NS4B, NS5A and NS5B (Okamoto *et al.*, 2004; Reed & Rice, 2000).

HCV NS5A is part of the replication complex that catalyses replication of the viral genome. NS5A takes two forms, p56 and p58, with different degrees of phosphorylation, which may play distinct roles in the virus replication cycle (Evans

†These authors contributed equally to this work.

‡Present address: Division of Microbiology, Department of Pathological Sciences, Faculty of Medical Sciences, University of Fukui, Fukui 910-1193, Japan.

et al., 2004; Song *et al.*, 1999). The SNARE-like membrane fusion proteins VAP-A and VAP-B have been reported to interact with NS5A, and the binding capacity is inversely correlated to the degree of NS5A phosphorylation (Evans *et al.*, 2004; Gao *et al.*, 2004; Hamamoto *et al.*, 2005). NS5A binds to and inhibits double-stranded RNA-dependent protein kinase (PKR) (Gale *et al.*, 1998) and 2′,5′-oligoadenylate synthetase (Taguchi *et al.*, 2004). NS5A seems to have the potential to regulate not only interferon responses but also many other cellular functions, such as mitogenic signalling, apoptosis, the cell cycle and reactive oxygen species signalling, by interacting with a variety of host proteins (Macdonald *et al.*, 2004). These NS5A-interacting proteins include SRCAP (Ghosh *et al.*, 2000), Grb2 (He *et al.*, 2002; Tan *et al.*,1999), p53 (Majumder *et al.*, 2001; Qadri *et al.*, 2002), phosphatidylinositol 3-kinase p85 subunit (He *et al.*, 2002; Street *et al.*, 2004), karyopherin β3 (Chung *et al.*, 2000), apolipoprotein A1 (Shi *et al.*, 2002), amphiphysin II (Zech *et al.*, 2003) and Src family protein tyrosine kinases (Macdonald & Harris, 2004; Macdonald *et al.*, 2004).

The non-receptor protein tyrosine kinase Syk is widely expressed in cells of the haematopoietic lineage, endothelium, epithelium and hepatocytes (Coopman *et al.*, 2000; Sada *et al.*, 2001; Tsuchida *et al.*, 2000; Turner *et al.*, 2000; Yanagi *et al.*, 1995, 2001). Syk contains tandem SH2 and kinase domains that are connected by an inter-SH2 domain and a linker region (Taniguchi *et al.*, 1991). The tandem SH2 domains of Syk bind to diphosphorylated immunoreceptor tyrosine-based activation motifs [ITAMs: YXX(L/I)X_{6-8}YXX(L/I)] in the cytoplasmic tail of the Fc receptor γ-chain or B-cell receptor subunit Igα to be activated after the engagement of immune receptors (Kurosaki *et al.*, 1995; Sada *et al.*, 2001; Shiue *et al.*, 1995; Turner *et al.*, 1995; Weiss & Littman, 1994). Autophosphorylation of Syk on Tyr^{525} and Tyr^{526} in the activation loop of the kinase domain results in an increase in its intrinsic kinase activity to phosphorylate its downstream signalling molecules, such as phospholipase C (PLC)-γ (Kurosaki *et al.*, 1995). Autophosphorylation on Tyr^{352} in the linker region is required for tyrosine phosphorylation of PLC-γ1 (Law *et al.*, 1996). Genetic studies have demonstrated that Syk is required for the development and maturation of B cells, mast-cell activation and platelet aggregation (Cheng *et al.*, 1995; Costello *et al.*, 1996; Poole *et al.*, 1997; Turner *et al.*, 1995, 2000). Furthermore, it has been reported that Syk functions as a tumour suppressor in breast cancers and that loss of Syk expression appears to be associated with malignant phenotypes (Coopman *et al.*, 2000).

In the present study, we demonstrated that HCV NS5A interacts physically with Syk to inhibit its kinase activity in human hepatoma-derived Huh-7 cells. Our results indicate that NS5A-induced downregulation of the possible tumour suppressor Syk may play a role in malignant transformation of HCV-infected hepatocytes.

METHODS

Expression plasmids. Mammalian expression plasmids for each of the Myc-tagged HCV proteins were constructed by amplifying and subcloning the corresponding cDNA fragments of pFK5B/2884Gly (Lohmann *et al.*, 2001) in frame to the pEF1/Myc-His(−) vector (Invitrogen). pFK5B/2884Gly was a kind gift from Dr R. Bartenschlager (University of Heidelberg, Germany). An expression plasmid for a polyprotein consisting of NS3–NS5B was amplified from pFK5B/2884Gly and subcloned into pEF1/Myc-His(−). Deletion mutants of NS5A were also amplified by PCR and subcloned into pEF1/Myc-His(−). Point mutations in NS5A [Tyr^{118} to Phe (Y118F), Val^{121} to Ala (V121A)] were introduced into pEF1/NS5A-Myc-His(−) by site-directed mutagenesis. Human Syk cDNA was a gift from Dr B. Müller-Hilke (University of Rostock, Germany). cDNA fragments for FLAG-tagged truncated forms and the kinase-inactive form of Syk were generated by PCR. All mutant forms of FLAG-tagged Syk were subcloned into pcDNA3.1/Hygro(+) (Invitrogen).

Cells, HCV RNA replicon and virus. Huh-7 human hepatoma-derived cells were maintained in Dulbecco's modified Eagle's medium supplemented with 10 % heat-inactivated fetal calf serum (FCS). Huh-7.5 cells (Blight *et al.*, 2002) were kindly provided by Dr C. M. Rice (The Rockefeller University, USA). BJAB cells, a human B-cell line expressing endogenous Syk, were cultured in RPMI 1640 supplemented with 10 % FCS.

Huh-7.5 cells stably harbouring an HCV subgenomic RNA replicon were prepared by using pFK5B/2884Gly, as described previously (Hidajat *et al.*, 2005; Lohmann *et al.*, 2001; Taguchi *et al.*, 2004; Takigawa *et al.*, 2004).

The plasmid pFL-J6/JFH1 encoding the entire genome of the HCV J6/JFH-1 strain was kindly provided by Dr C. M. Rice, and cell-free virus was propagated in Huh-7.5 cell cultures, as described previously (Lindenbach *et al.*, 2005).

Protein expression. Protein expression was performed using a recombinant vaccinia virus expressing T7 RNA polymerase (vTF7-3), as described previously (Deng *et al.*, 2006; Muramatsu *et al.*, 1997). In some experiments, protein expression was performed using a plasmid-based expression system without vTF7-3. For BJAB cells, we used an electroporation method (Schneider & Kieser, 2004). In brief, 3×10^6 cells were washed once with PBS and incubated for 10 min with 15 μg plasmid DNA in 250 μl RPMI 1640. Electroporation was carried out in a 4 mm cuvette using a Bio-Rad Gene Pulser II with a capacity of 975 μF and a voltage of 180 V. Immediately after electroporation, 500 μl FCS was added to the cells, which were then transferred to 4.5 ml RPMI 1640.

To activate Syk under hyperosmolarity conditions, cells were incubated with serum-free medium containing 400 mM sorbitol for 30 min at 37 °C, as described previously (Miah *et al.*, 2004). In addition, cells were treated with sodium pervanadate (generated by mixing 0.1 mM Na_3VO_4 with 1 mM H_2O_2) for 30 min to activate Syk (Wienands *et al.*, 1996).

Immunohistochemistry. Human normal adult liver autopsy materials and surgically resected liver tissue of patients with HCV-associated HCC were obtained with written informed consent. The tissues were fixed with 10 % buffered formalin, embedded in paraffin and sectioned. Immunohistochemical staining was performed with a Dako EnVision+ kit, according to the manufacturer's instructions. In brief, fixed sections were depleted of paraffin by treatment with xylene, dehydrated in ethanol and incubated with 3 % H_2O_2 to quench endogenous peroxidase activity. After being autoclaved at 121 °C for 20 min, the sections were incubated with a blocking

solution and then with anti-Syk rabbit polyclonal antibody (N-19; Santa Cruz Biotech). Normal rabbit IgG served as a control. The sections were then incubated with horseradish peroxidase-labelled polymer-conjugated secondary antibody. The sections were counter-stained with haematoxylin and examined under a light microscope. To confirm the specificity of immunostaining, anti-Syk antibody was pre-incubated with a 1000-fold excess of blocking peptide (Santa Cruz Biotech) for 2 h at room temperature prior to staining.

Detection of HCV RNA by *in situ* RT-PCR. *In situ* RT-PCR was performed as described previously (Maeda *et al.*, 2004) with some modifications. Briefly, OCT-embedded frozen liver biopsy sections were fixed with 10% formaldehyde and treated with proteinase K. The samples were subjected to *in situ* reverse transcription using Moloney murine leukemia virus reverse transcriptase with an antisense primer for HCV (nt 290–272; 5′-AGTACCACAA GGCCTTTCG-3′), followed by *in situ* PCR using an *in situ* PCR System 1000 (Applied Biosystems) in the reaction mixture containing the antisense and a sense primer (nt 129–147; 5′-CCGGGAGAG CCATAGTGGT-3′). After being fixed in 4% paraformaldehyde, the PCR products were detected by *in situ* hybridization using a digoxigenin (DIG)-labelled oligonucleotide probe, 5′-(DIG)-ATTTGGGCTGTGCCCCCGCGAGACTGCTAGCCGAGTAGTGTT-GGGT-(DIG)$_n$-3′ (nt 225–270). Anti-DIG antibody conjugated with alkaline phosphatase (Roche) was used to detect the probe. The slides were incubated in a dye solution containing nitro blue tetrazolium, 5-bromo-4-chloro-3-indolylphosphate and levamizole to yield a purplish-blue precipitate.

Immunoprecipitation and Western blotting. Cultured cells were lysed with a buffer containing 1% Triton X-100, 50 mM Tris/HCl (pH 7.4), 150 mM NaCl, 10 mM EDTA, 1 mM NaF, 1 mM Na_3VO_4 and 1 mM PMSF. The lysate was centrifuged at 12000 *g* for 20 min at 4 °C and the supernatant was immunoprecipitated with appropriate antibodies. In the case of liver tissue, each tissue sample was placed in a tube containing glass beads (1 mm diameter; BioSpec Products) to which 1 ml lysis buffer was added. The tube was then shaken at 4 °C for 3 min using a Mini-BeadBeater (BioSpec Products) to homogenize the tissues. After centrifugation at 80 *g* for 3 min, the supernatant was collected for immunoprecipitation analysis.

Immunoprecipitation and Western blot analyses were performed as described previously (Deng *et al.*, 2006). In brief, the supernatants of the lysates were pre-cleared with control IgG and protein G–Sepharose 4 Fast Flow (GE Healthcare) and incubated with appropriate antibodies at 4 °C for 1 h, followed by incubation with protein G–Sepharose 4 Fast Flow for another 1 h. After six washes with lysis buffer, the immunoprecipitates were analysed by Western blotting.

Antibodies used were as follows: anti-FLAG rabbit polyclonal antibody (Sigma); anti-Myc polyclonal and monoclonal antibodies (Santa Cruz Biotech); anti-Syk monoclonal antibody (4D10; Santa Cruz Biotech); anti-phospho Syk(Tyr^{352}) and Syk(Tyr$^{525/526}$) rabbit polyclonal antibodies (Cell Signaling Technology); anti-PLC-γ1 monoclonal antibody (BD Biosciences); mouse monoclonal antibodies against core (Yasui *et al.*, 1998), NS3, NS4A and NS5A (kind gifts from Dr I. Fuke, Osaka University, Japan); anti-NS5A rabbit polyclonal antibody (NS5ACL1; a kind gift from Dr K. Shimotohno, Kyoto University, Japan; Miyanari *et al.*, 2007); and anti-NS5B goat polyclonal antibody (sc-17532; Santa Cruz Biotech). Normal IgG served as a control.

***In vitro* protein kinase assay.** An *in vitro* protein kinase assay was performed as reported previously (Miah *et al.*, 2004; Sada *et al.*, 2000, 2001). In brief, immunoprecipitates obtained with anti-Syk antibody from differentially transfected cells were incubated with 10 μg H2B histone (Sigma) as substrate in 20 μl kinase buffer, composed of 30 mM HEPES (pH 7.5), 10 mM $MgCl_2$, 2 mM $MnCl_2$, 4 μM ATP and 4 μCi (148 kBq) [γ-^{32}P]ATP, for 30 min at room temperature. Reactions were terminated by boiling for 5 min in 2× sample buffer.

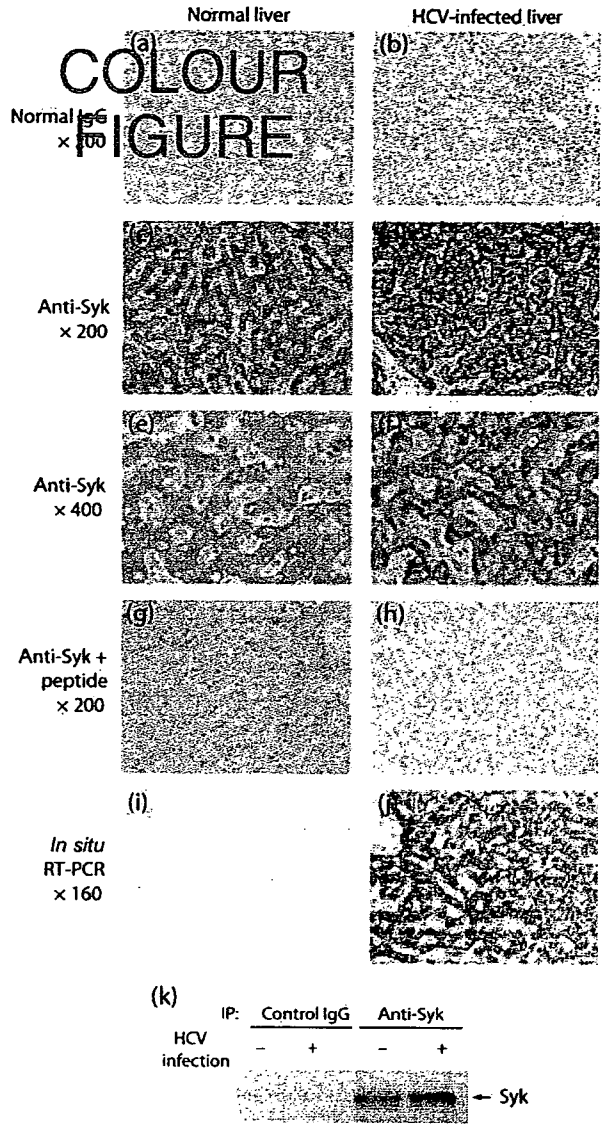

Fig. 1. Endogenous Syk expression in human liver tissues *in vivo*. Normal liver tissues (a, c, e, g, i) and HCV-infected non-cancerous liver tissues (b, d, f, h, j) were analysed. Formalin-fixed samples were stained with control IgG (a, b) or anti-Syk polyclonal antibody without (a–f) or with (g, h) pre-incubation with an excess amount of the immunogenic peptides. Frozen tissues were sectioned and examined for the presence of HCV RNA by *in situ* RT-PCR (i, j). Representative results are shown from four normal livers and ten HCV-infected livers. (k) Western blot analysis of normal human liver and HCV-infected non-cancerous liver. Supernatants of liver tissue homogenates (1.75 mg protein equivalent) were immunoprecipitated with anti-Syk monoclonal antibody (4D10) and probed with the same antibody or with control IgG.

Proteins were separated by SDS-PAGE. The gels were treated with 1 M KOH for 1 h at 56 °C to remove phosphoserine and most of the phosphothreonine. After gel drying, radiolabelled proteins were visualized by autoradiography. For quantitative analysis, γ-^{32}P incorporation was measured using a PhosphorImager (BAS2000; Fuji) and protein amounts with an LAS1000 image analyser (Fuji).

RESULTS

Different expression patterns of endogenous Syk in normal and HCV-infected liver tissues

We first examined whether Syk was expressed in human liver tissues. Immunohistochemical analysis revealed that Syk was indeed expressed and rather diffusely distributed throughout the cytoplasm of normal adult hepatocytes (Fig. 1c, e). This pattern was observed with four out of four normal liver tissues (100%; data not shown). The specificity of the staining was verified by pre-incubating the antibody with an excess amount of the immunogenic peptides (Fig. 1g, h). We then examined Syk expression in non-cancerous liver tissue obtained from patients with HCV-associated HCC. Interestingly, Syk was detected near the plasma membrane with a patchy pattern in hepatocytes of eight out of ten HCV-infected patients (80%; Fig. 1d, f, and data not shown). All of the specimens stained with normal rabbit IgG were negative (Fig. 1a, b). We confirmed that almost all off the hepatocytes in the tissue samples were infected with HCV using *in situ* RT-PCR (Fig. 1i, j).

Western blot analysis confirmed Syk expression in human liver tissue, irrespective of HCV infection (Fig. 1k). It should be noted, however, that the Syk expression was rather weak, as we could achieve successful Western blotting only after the tissue lysates were concentrated by immunoprecipitation with specific antibody. Also, possibly due to the low level of expression and comparatively low sensitivity of the antibodies used for Western blotting, we could not detect the phosphorylated forms of Syk in the liver tissue (data not shown).

Identification of Syk as a novel NS5A-interacting protein

We then examined the possible interaction between HCV proteins and Syk in cultured cells. For this purpose, various HCV proteins and Syk were expressed ectopically in Huh-7 cells, as these cells do not express endogenous Syk. Co-immunoprecipitation analysis revealed that NS5A associated with Syk, whereas the other HCV proteins associated with Syk very weakly or not at all (Fig. 2a, b). A specific interaction of NS5A with Syk was also observed when NS5A was expressed as part of an NS3–NS5B polyprotein (Fig. 2c). These results collectively suggested that NS5A interacts specifically with Syk.

Next, we examined the possible interaction of NS5A with endogenously expressed Syk. As human hepatoma-derived cell lines, such as Huh-7, HepG2 and FLC4, are negative for endogenous Syk expression, we used BJAB cells endogenously expressing Syk. Unlike ectopically expressed Syk, endogenous Syk in BJAB cells is not tyrosine phosphorylated. Therefore, we treated the cells with pervanadate to induce tyrosine phosphorylation of Syk. Co-immunoprecipitation experiments clearly demonstrated that NS5A

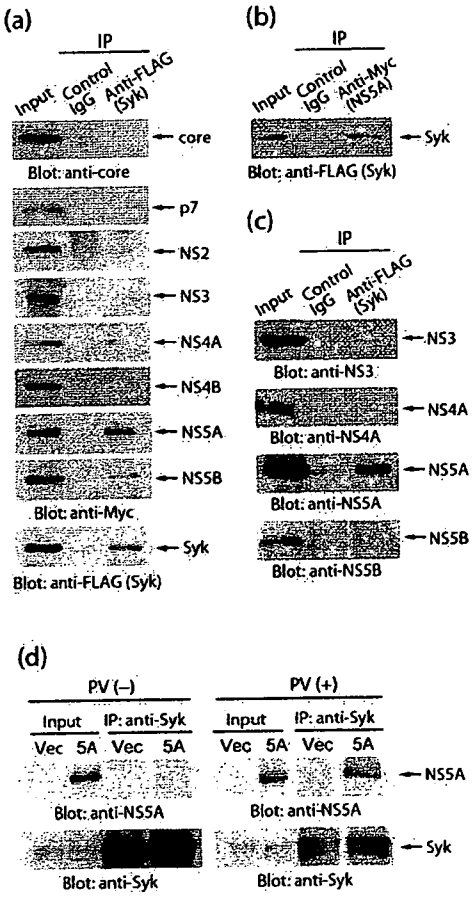

Fig. 2. NS5A specifically interacts with Syk in Huh-7 cells. (a) Each of the Myc-tagged HCV proteins was expressed with FLAG-tagged full-length Syk. Cell lysates were immunoprecipitated using anti-FLAG antibody or control IgG. Cell lysates (input) and the immunoprecipitates were probed with anti-core or anti-Myc antibodies. A representative result verifying efficient immunoprecipitation is shown at the bottom. (b) Myc-tagged NS5A was expressed with FLAG-tagged full-length Syk. Cell lysates were immunoprecipitated using anti-Myc antibody or control IgG, and probed with anti-FLAG antibody. (c) A polyprotein consisting of NS3–NS5B was expressed with FLAG-tagged Syk. Cell lysates were immunoprecipitated with anti-FLAG antibody or control IgG, and probed with the indicated antibodies. (d) NS5A was expressed in BJAB cells expressing endogenous Syk. The cells were treated with pervanadate (PV) or left untreated. Cell lysates were immunoprecipitated with anti-Syk monoclonal antibody and probed with anti-NS5A or anti-Syk monoclonal antibody. Vec, control using empty vector.

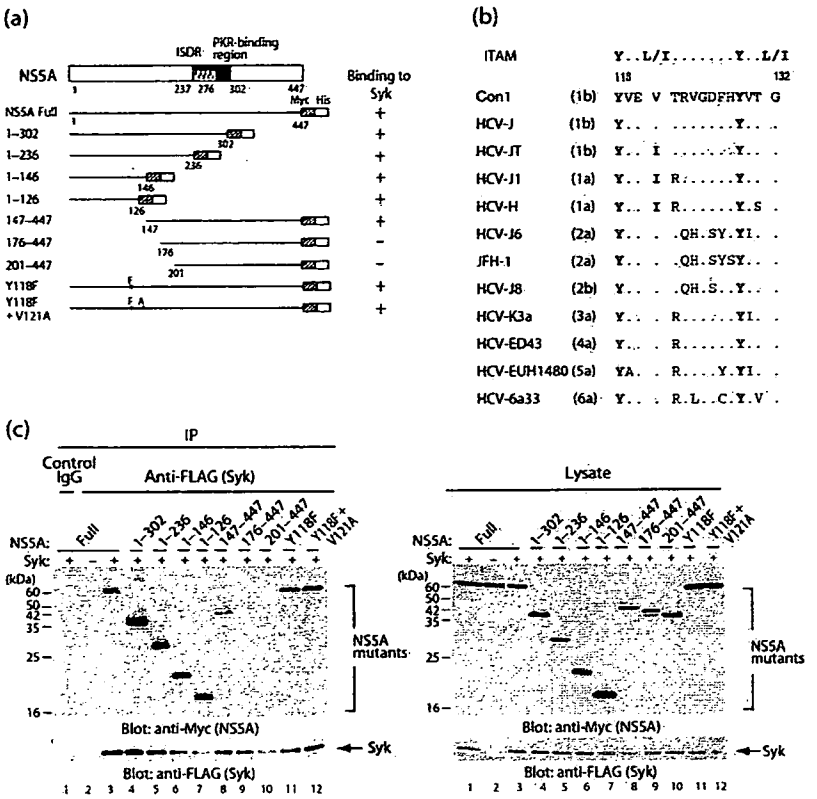

Fig. 3. Determination of the Syk-binding region(s) of NS5A. (a) Schematic diagram of various deletion mutants of NS5A and their Syk-binding capacity. (b) Alignment of amino acid sequences surrounding the ITAM-related sequence in NS5A of various HCV strains. The genotype is indicated in parentheses. Residues identical to those of HCV strain Con1 are shown by a dot. Residues identical to ITAM are shown in bold. (c) Full-length (Full) and a series of deletion mutants of Myc-tagged NS5A were expressed in Huh-7 cells with or without FLAG-tagged full-length Syk. Cell lysates were immunoprecipitated using anti-FLAG antibody and probed with anti-Myc antibody (left panel). Efficient immunoprecipitation was verified (bottom). Cell lysates were probed directly with anti-Myc and anti-FLAG antibodies to verify comparable expression levels of the NS5A mutants and Syk, respectively (right panels).

interacted with endogenous Syk when the cells were treated with pervanadate, but not when the cells were left untreated (Fig. 2d).

The N-terminal region of NS5A is required for interaction with Syk

To map a Syk-interacting region(s) of NS5A, interaction between various deletion mutants of NS5A and Syk was tested. C-terminally deleted mutants of NS5A up to aa 126, as well as the full-length NS5A, were co-immunoprecipitated with Syk (Fig. 3a, c). This result suggested that neither the PKR-binding region nor the interferon sensitivity-determining region (ISDR) of NS5A was required for the interaction with Syk. A proline-rich region of NS5A (aa 343–356), which is reported to bind to the Src family kinases (Macdonald & Harris, 2004; Macdonald *et al.*, 2004), was not involved in the Syk interaction either. In contrast, the N-terminally truncated mutant of NS5A(147–447), but not the further truncated mutants NS5A(176–447) or NS5A(201–447), was co-immunoprecipitated with Syk, suggesting that a region of NS5A between aa 147 and 175 is also involved in the interaction with Syk. We also observed that NS5A(1–126) and NS5A(174–447), but not NS5A(201–447), interacted with Syk(1–261) or Syk(379–635) (data not shown). These results collectively suggested that NS5A interacts with Syk through two independent regions of NS5A (aa 1–126 and 147–175).

Syk is activated by interaction with a diphosphorylated ITAM of immune receptors (Sada *et al.*, 2001; Turner *et al.*, 2000; Weiss & Littman, 1994). NS5A from HCV strain Con1 possesses a sequence (AEEY^{118}VEV^{121}-TRVGDFHY^{129}VTG) that resembles an ITAM (Fig. 3b). We found that the two tyrosine residues at positions 118 and 129 are highly conserved across different genotypes and subtypes. The tyrosine at position 118 is exposed on

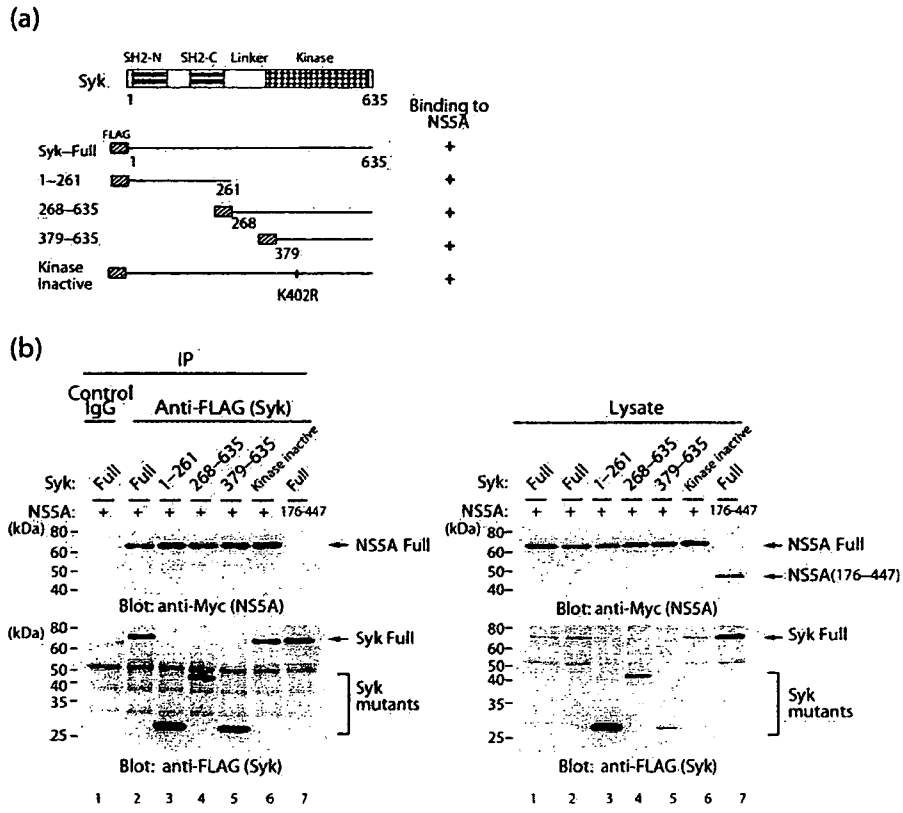

Fig. 4. NS5A interacts with both N-terminal and C-terminal regions of Syk. (a) Schematic diagram of the deletion mutants of Syk and their NS5A-binding capacity. (b) Full-length (Full) and a series of domain-deletion mutants of FLAG-tagged Syk was expressed in Huh-7 cells with Myc-tagged full-length NS5A (lanes 1–6) or NS5A(176–447) (lane 7). Cell lysates were immunoprecipitated using anti-FLAG antibody and probed with anti-Myc antibody (left upper panel). Efficient immunoprecipitation of Syk deletion mutants was verified (bottom). Cell lysates were probed directly with anti-Myc and anti-FLAG antibodies to verify comparable expression levels of the NS5A and Syk mutants, respectively (right panels).

the surface of the NS5A molecule (Tellinghuisen *et al.*, 2005). We examined whether this sequence motif was involved in the interaction with Syk. A single point mutation of Tyr^{118} (Y118F) or double mutations of Tyr^{118} and Val^{121} (Y118F and V121A) in NS5A did not affect the interaction with Syk (Fig. 3c, lanes 11 and 12). Thus, it is unlikely that NS5A binds to Syk through its ITAM-related sequence in the same manner as that observed for immune receptors.

To map the NS5A-binding region in Syk, a series of domain-deleted mutants of Syk was examined. The results obtained revealed that both N-terminal (tandem SH2 domains) and C-terminal halves (linker and the kinase domain) interacted with NS5A (Fig. 4). The kinase domain alone and a kinase-inactive form of Syk were also co-immunoprecipitated with NS5A. These results suggested that the NS5A–Syk interaction occurs through the N- and C-terminal regions of Syk and that the catalytic activity of Syk is not necessary for the interaction.

NS5A expression downregulates the kinase activity of Syk

Next, we tested the possible effect of NS5A expression on Syk kinase activity. An *in vitro* kinase assay revealed that full-length NS5A and a C-terminally deleted NS5A(1–302) mutant significantly inhibited Syk kinase activity (Fig. 5, lanes 2–4). In contrast, NS5A(1–236), which lacked both the PKR-binding region (aa 237–302) and ISDR (aa 237–276), failed to inhibit Syk kinase activity, although it could interact with Syk. NS5A(176–447), which contained the PKR-binding region and ISDR but lacked the Syk-binding region, did not affect Syk kinase activity. These results collectively suggested that NS5A requires both N-terminal (aa 1–175) and central (aa 237–302) regions for the downregulation of Syk kinase activity (Table 1).

To address the relevance of the interaction between NS5A and Syk, the possible effect(s) of NS5A on Syk-mediated cellular signalling in Huh-7 cells was examined. Ectopic

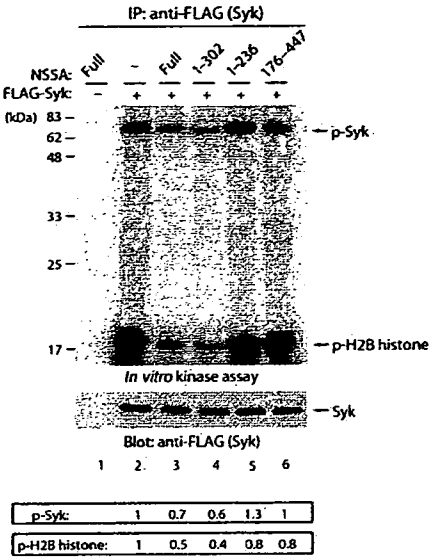

Fig. 5. NS5A downregulates Syk kinase activity. Myc-tagged NS5A and FLAG-tagged Syk were expressed in Huh-7 cells. Cell lysates were immunoprecipitated with anti-FLAG antibody and the immunoprecipitates were subjected to an *in vitro* kinase assay using H2B histone as substrate. Phosphorylation of Syk (p-Syk) and H2B histone (p-H2B histone) was visualized by autoradiography (upper panel). Efficient immunoprecipitation of Syk was verified (lower panel). Arbitrary units of Syk kinase activities, represented by the phosphorylation values of p-Syk and p-H2B histone normalized to the amounts of immunoprecipitated Syk, are shown at the bottom.

expression of Syk alone mediated signal transduction to induce tyrosine phosphorylation of a wide variety of cellular proteins, either directly or indirectly (Fig. 6a, lanes 1 and 3). Hyperosmolarity stress (400 mM sorbitol treatment) enhanced Syk-mediated tyrosine phosphorylation of cellular proteins (Fig. 6a, lanes 3 and 4), with the result being consistent with the previous observation (Miah *et al.*, 2004). Interestingly, co-expression of NS5A decreased Syk-mediated tyrosine phosphorylation of cellular proteins both in the absence and presence of hyperosmolarity stress (Fig. 6a, lanes 7 and 8). The phosphorylation of Syk on Tyr^{352} and/or $Tyr^{525/526}$ is a marker for Syk activation. Using these parameters, we confirmed that co-expression of NS5A inhibited Syk activation both in the absence and presence of hyperosmolarity stress (Fig. 6b).

PLC-γ1 has been reported to be a downstream molecule of Syk-mediated signal transduction (Law *et al.*, 1996). Our results demonstrated that NS5A inhibited PLC-γ1 phosphorylation, probably through downregulation of Syk kinase activity, both in the absence and presence of hyperosmolarity stress (Fig. 6c).

Table 1. Summary of NS5A deletion mutational analysis of the interaction with Syk and inhibition of Syk kinase activity

NS5A mutant	Interaction with Syk	Inhibition of Syk
NS5A(1–447; full)	+	+
NS5A(1–302)	+	+
NS5A(1–236)	+	–
NS5A(176–447)	–	–

NS5A expressed in the context of HCV RNA replication interacts with Syk in Huh-7.5 cells

The interaction of NS5A with Syk was examined further using Huh-7.5 cells harbouring an HCV subgenomic RNA replicon. The results obtained clearly demonstrated that NS5A expressed in the context of HCV RNA replication interacted with Syk (Fig. 7a). It is well known that NS5A takes two forms, p56 and p58, with the former being the basally phosphorylated form and the latter the hyperphosphorylated form (Kaneko *et al.*, 1994; Song *et al.*, 1999). It is noteworthy that Syk interacted with p56 more efficiently than with p58.

We also examined the interaction of NS5A with Syk in Huh-7.5 cells infected with the J6/JFH-1 strain of HCV. The results demonstrated that NS5A interacted with Syk in HCV-infected cells (Fig. 7b). These results collectively suggested that the NS5A–Syk interaction occurs in the context of virus replication, where NS5A is primarily utilized to form the viral replication complex. In this connection, HCV J6/JFH-1 replication was not affected significantly by ectopically expressed Syk in Huh-7.5 cells (data not shown). This observation, however, does not necessarily exclude the possibility that the NS5A interaction with Syk exerts certain biological effect(s) on the host cell's fate.

Syk kinase activity is suppressed in the context of HCV RNA replication

We then examined Syk kinase activity in the HCV subgenomic RNA-harbouring Huh-7.5 cells. An *in vitro* kinase assay demonstrated that Syk kinase activities, represented by autophosphorylation of Syk (p-Syk) and phosphorylation of a substrate (p-H2B histone), were significantly suppressed in HCV RNA-replicating cells compared with the control (Fig. 7c). These results suggested the possibility that Syk kinase activity is downregulated through an NS5A–Syk interaction in HCV-infected hepatocytes as well.

DISCUSSION

The non-receptor protein tyrosine kinase Syk is expressed in a wide variety of haematopoietic cell lineages (Taniguchi *et al.*, 1991). It is also expressed in human mammary

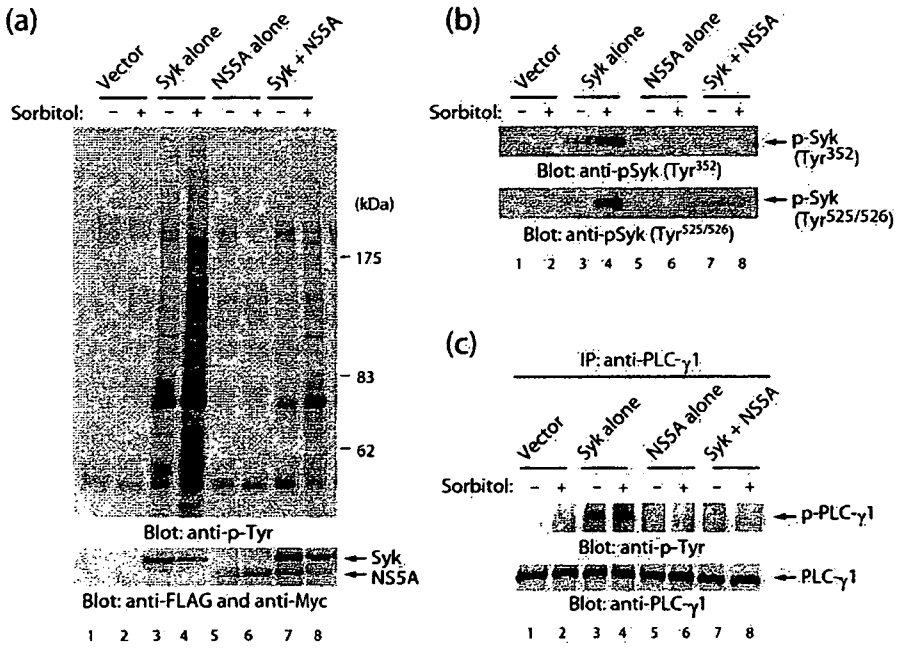

Fig. 6. NS5A suppresses hyperosmolarity stress-induced Syk-mediated tyrosine phosphorylation of cellular proteins. (a) Myc-tagged NS5A was expressed in Huh-7 cells with or without FLAG-tagged Syk. The cells were incubated with or without 400 mM sorbitol for 30 min and then lysed in lysis buffer. Half of the cell lysate was probed with anti-phosphotyrosine (p-Tyr) antibody (upper panel) and the remaining half with anti-FLAG and anti-Myc antibodies (bottom). (b) Cell lysates were probed with anti-p-Syk(Tyr^{352}) (upper panel) or anti-p-Syk($Tyr^{525/526}$) antibody (lower panel). (c) Cell lysates were immunoprecipitated using anti-PLC-γ1 antibody and probed with anti-p-Tyr antibody (upper panel). Efficient immunoprecipitation of PLC-γ1 was verified (lower panel).

(Coopman *et al.*, 2000) and airway epithelial cells (Ulanova *et al.*, 2005), nasal fibroblasts (Yamada *et al.*, 2001) and hepatocytes (Tsuchida *et al.*, 2000). These results suggest that Syk plays a general physiological role in non-haematopoietic cells as well. The first report of Syk having a role in cancer was a study of mammary epithelial cells (Coopman *et al.*, 2000). Since then, there have been several reports that Syk functions as a tumour suppressor in the process of malignant tumour development, such as gastric cancer (Wang *et al.*, 2004) and leukaemia (Goodman *et al.*, 2001). To look into the possible relevance of Syk in HCV-infected hepatocytes and also the possible involvement of Syk in HCC development, we first examined Syk expression in hepatocytes obtained from HCV-infected and uninfected subjects. We found that Syk was expressed near the plasma membrane of hepatocytes of HCV-infected patients, with a patchy pattern, whereas it was expressed rather diffusely in the cytoplasm of normal, uninfected hepatocytes (Fig. 1).

We also demonstrated that NS5A interacted with Syk and inhibited its kinase activity when expressed ectopically in Huh-7 cells (Figs 2, 5 and 6). The NS5A interaction with Syk was observed even in the context of HCV RNA replication (Fig. 7a, b) and Syk kinase activity was inhibited in HCV RNA replicon-harbouring cells (Fig. 7c). It is likely, therefore, that Syk is a binding partner of NS5A and is functionally inhibited in HCV-infected hepatocytes as well. Whilst an N-terminal portion of NS5A (aa 1–175) was responsible for the binding to Syk, a central portion (aa 237–302) was also required for the inhibition of Syk kinase activity (Figs 3 and 5). It has been reported that NS5A associates with the non-receptor protein tyrosine kinases Lyn and Fyn, members of the Src family kinases, through the proline-rich region of NS5A (aa 343–356) and the SH3 domain of the kinases, thereby inhibiting and activating the kinase activities of Lyn and Fyn, respectively (Macdonald & Harris, 2004; Macdonald *et al.*, 2004). In contrast, Syk does not possess an SH3 domain but has two tandem SH2 domains. These SH2 domains are known to interact with diphosphorylated ITAM of immune receptors, resulting in activation of Syk in an autocrine or paracrine manner (Sada *et al.*, 2001; Yanagi *et al.*, 1995). However, it is unlikely that the NS5A–Syk interaction occurs through its ITAM-related sequence in the same manner as that observed for immune receptors, as NS5A mutants with a mutated ITAM-like sequence still interacted with Syk (Fig. 3). Also, the SH2 domains of Syk are not the only binding sites for NS5A (Fig. 4). These results suggest that the mechanism

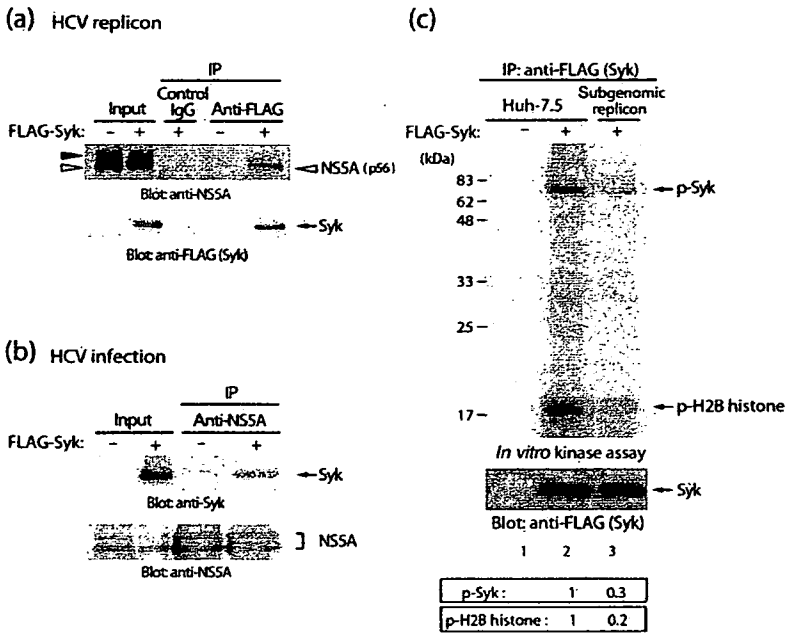

Fig. 7. NS5A expressed in the context of HCV RNA replication interacts with Syk and inhibits its kinase activity. (a) FLAG-tagged Syk was expressed in HCV RNA replicon-harbouring Huh-7.5 cells. Cell lysates were immunoprecipitated with anti-FLAG antibody or control IgG and probed with anti-NS5A (upper panel) or anti-FLAG antibody (lower panel). Filled and open arrowheads indicate the hyperphosphorylated (p58) and hypophosphorylated forms of NS5A (p56), respectively. (b) FLAG-tagged Syk was expressed in HCV J6/JFH-1-infected Huh-7.5 cells. Cell lysates were immunoprecipitated with anti-NS5A polyclonal antibody and probed with anti-Syk monoclonal antibody. (c) FLAG-tagged Syk was expressed in HCV RNA replicon-harbouring Huh-7.5 cells. Cell lysates were immunoprecipitated with anti-FLAG antibody and the immunoprecipitates were subjected to an *in vitro* kinase assay using H2B histone as substrate. Phosphorylation of Syk (p-Syk) and H2B histone (p-H2B histone) was visualized by autoradiography (upper panel). Efficient immunoprecipitation of Syk was verified (lower panel). Arbitrary units of Syk kinase activities, represented by the phosphorylation values of p-Syk and p-H2B histone normalized to the amounts of immunoprecipitated Syk, are shown at the bottom.

underlying the NS5A–Syk interaction differs from what has been observed for Syk and its interacting proteins in immune cells. It is possible that multiple regions of NS5A are involved in the interaction with Syk. Alternatively, NS5A may interact with Syk indirectly through the other host protein(s) that binds directly to Syk.

Syk is activated by cytokine stimulation, hyperosmolarity shock, oxidative stress and engagement with integrin (Corey *et al.*, 1994; Gao *et al.*, 1997; Miah *et al.*, 2004). However, the biological relevance of Syk in hepatocytes has not yet been demonstrated. We have shown in the present study that hyperosmolarity stress-induced activation of Syk resulted in increased tyrosine phosphorylation of endogenous PLC-γ1 (Fig. 6c). This result suggests that activated Syk sends signals to PLC-γ1 in hepatocytes, as observed in immune cells (Law *et al.*, 1996). Our findings that NS5A associates with Syk strongly suggest that NS5A affects the Syk signalosome to alter the signal transduction elicited by the Syk–PLC-γ1 interaction.

Phosphorylation of tyrosine residues in the linker region of Syk is required for immune receptor signalling. Genetic studies have demonstrated that phosphorylation of Tyr^{348} and Tyr^{352} in the linker region of Syk is involved in regulating tyrosine phosphorylation of LAT (linker for activating T cells), SLP-76 and PLC-γ1 and -γ2, and affects Ca^{2+} mobilization triggered by aggregation of the high-affinity IgE receptor (Simon *et al.*, 2005; Zhang *et al.*, 2002). We observed that NS5A downregulated phosphorylation of Tyr^{352} of Syk (Fig. 6b), which correlated with the inhibition of Syk kinase activity. The phosphorylation state of Tyr^{352} also correlated well with the tyrosine phosphorylation state of PLC-γ1. This suggests the possibility that Ca^{2+} mobilization is affected in HCV-infected hepatocytes through the NS5A-mediated downregulation of Tyr^{352} phosphorylation on Syk.

Unlike ectopically expressed Syk, endogenously expressed Syk in B cells under normal conditions is not tyrosine phosphorylated (Wienands *et al.*, 1996). Pervanadate stimulation is known to induce tyrosine phosphorylation of endogenous Syk. We examined the possible interaction of endogenous Syk and NS5A. Our results demonstrated that NS5A interacted with endogenous Syk when the cells were treated with pervanadate, but not when the cells were left untreated (Fig. 2d). These results suggest that NS5A interacts with the tyrosine-phosphorylated, active form of Syk.

Whilst Syk is commonly expressed in normal human breast tissues, benign breast lesions and low-tumorigenic breast